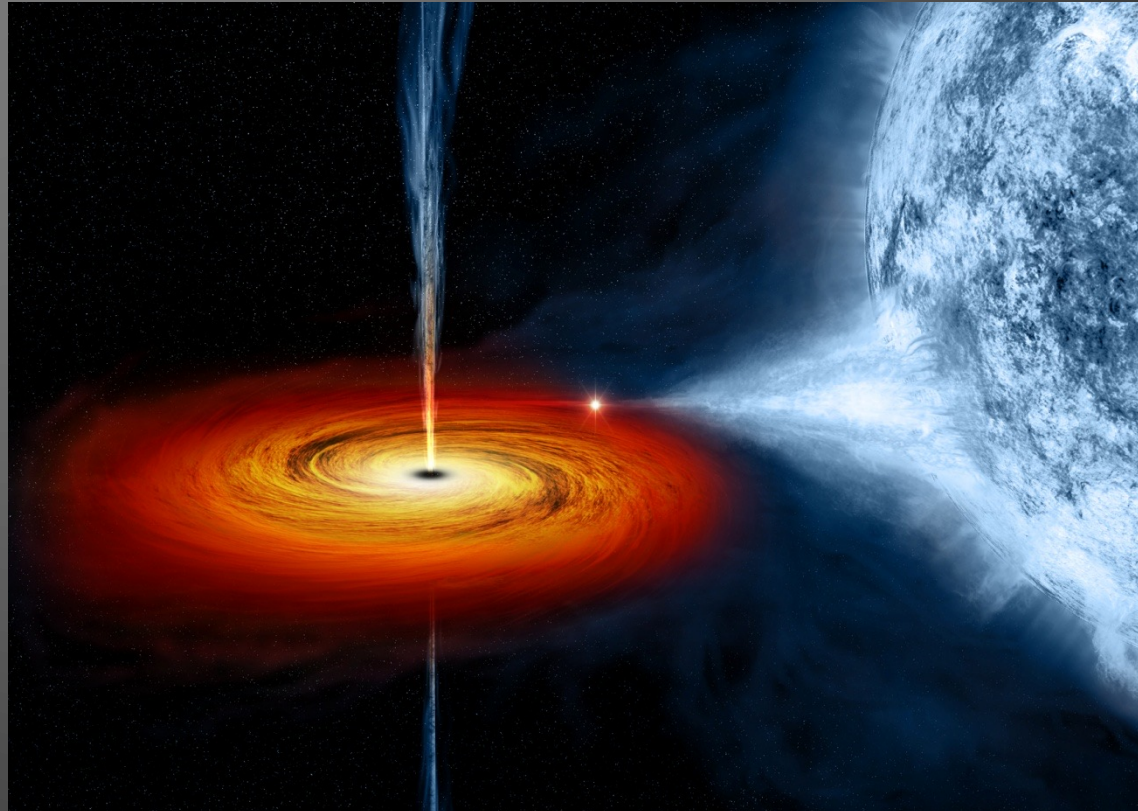


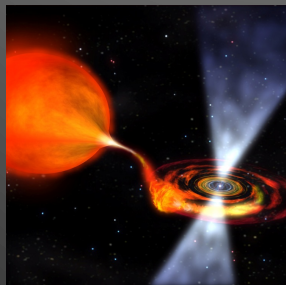
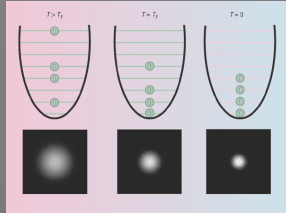
PHYSICS OF COMPACT OBJECTS AND THEIR BINARY INTERACTIONS



AALBORG
UNIVERSITY

Thomas Tauris – Physics, Aalborg University

Programme



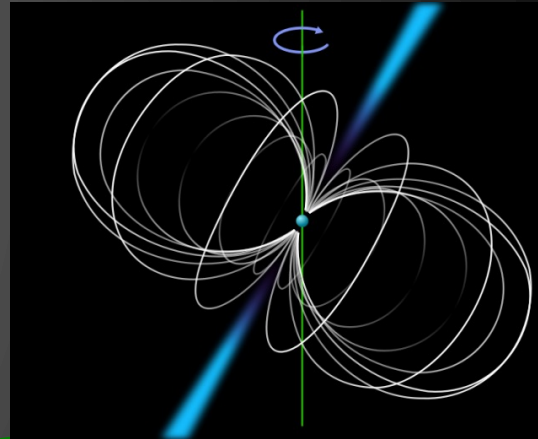
- * Introduction**
- * Degenerate Fermi Gases**
 - Non-relativistic and extreme relativistic electron / (n,p,e⁻) gases
- * White Dwarfs**
 - Structure, cooling models, observations
- * Neutron Stars**
 - Structure and equation-of-state
- * Radio Pulsars**
 - Characteristics, spin evolution, magnetars, observations
- * Binary Evolution and Interactions**
 - X-ray binaries, accretion, formation of millisecond pulsars, recycling
- * Black Holes**
 - Observations, characteristics and spins
- * Gravitational Waves**
 - Sources and detection, kilonovae
- * Exam**

Last time

Radio Pulsars

Characteristics, observations, spin evolution, magnetars

- Observational aspects of radio pulsars
 - The radio pulsar population in the Milky Way
 - Pulse profiles / Scintillation / Dispersion measure
 - Emission properties
- Spin evolution of pulsars in the $P\dot{P}$ -diagram
 - The magnetic dipole model
 - Evolution with B-field decay
 - Evolution with gravitational wave emission
 - The braking index
 - True ages of radio pulsars
- Magnetars
 - Soft gamma-ray repeaters (SGRs) and Anomalous X-ray pulsars (AXPs)



Blackboard

X-ray Binaries

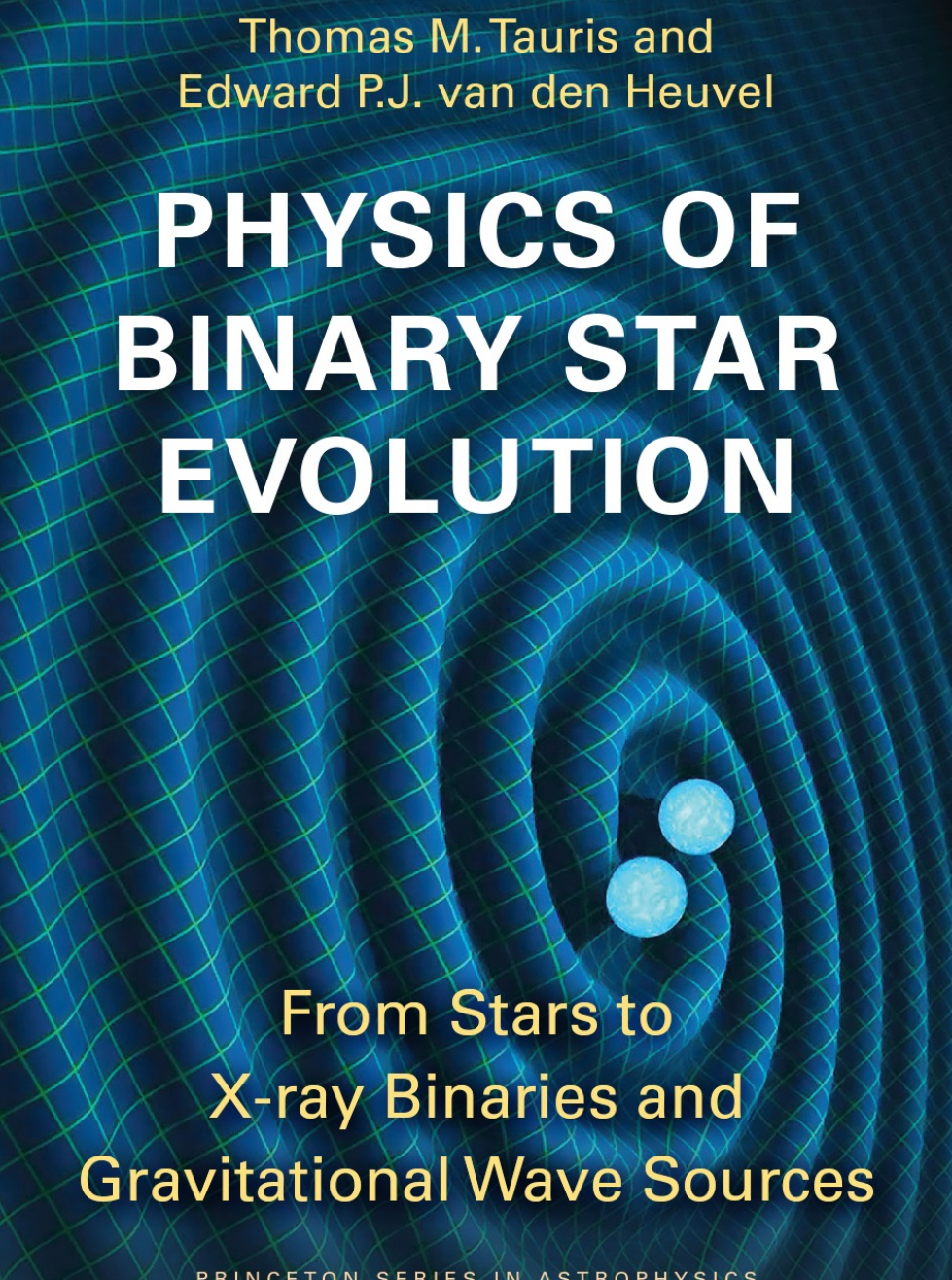


- X-ray binaries (HMXBs / LMXBs)
- Roche-lobe overflow - Cases A, B, C, and Case BB
- Stability criteria for mass transfer / stellar evolution
- Orbital angular momentum balance equation
- Common envelope and spiral-in evolution

**For a review: Tauris & van den Heuvel (2006)
and new textbook: Tauris & van den Heuvel (2023)**

Thomas M. Tauris and
Edward P.J. van den Heuvel

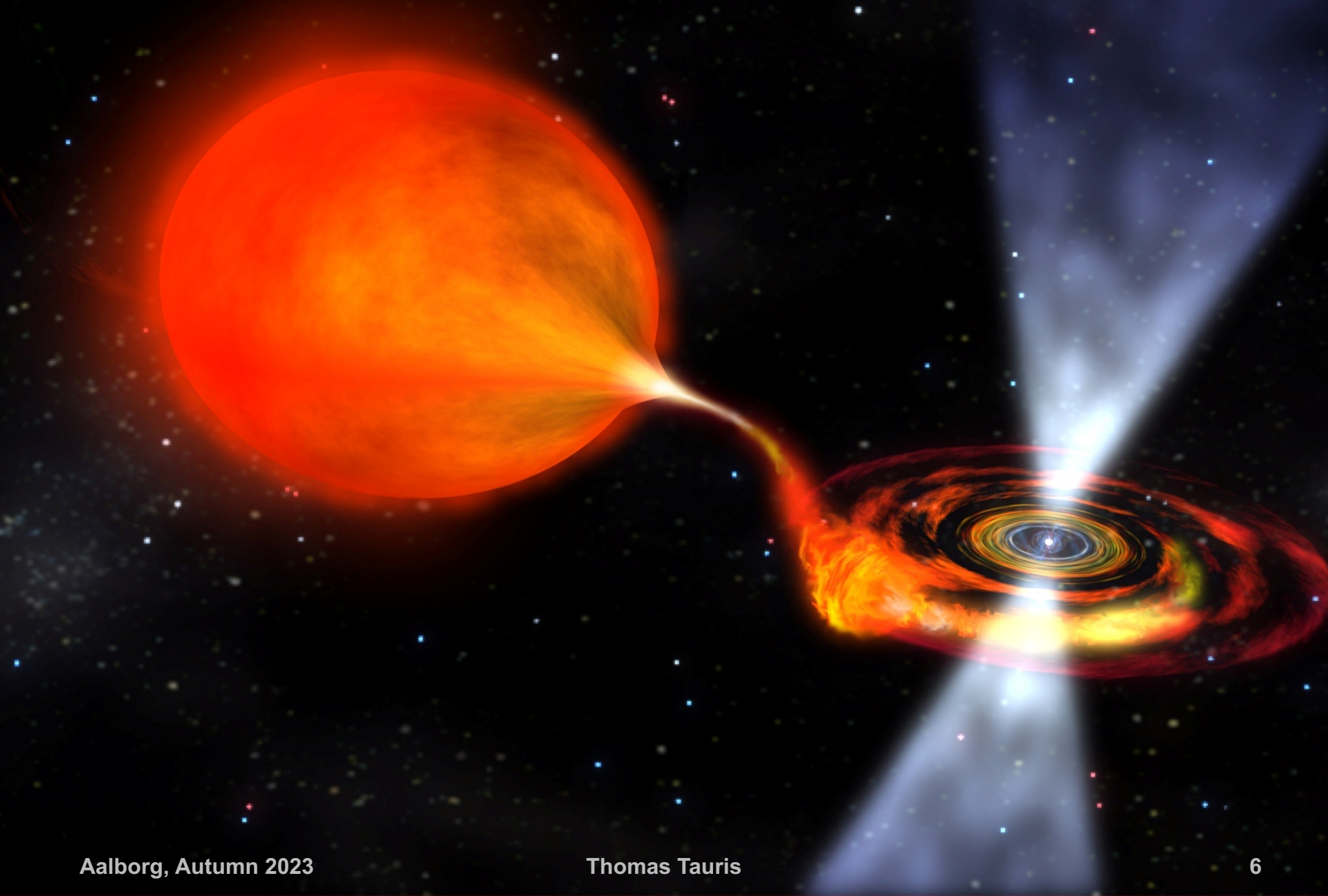
PHYSICS OF BINARY STAR EVOLUTION



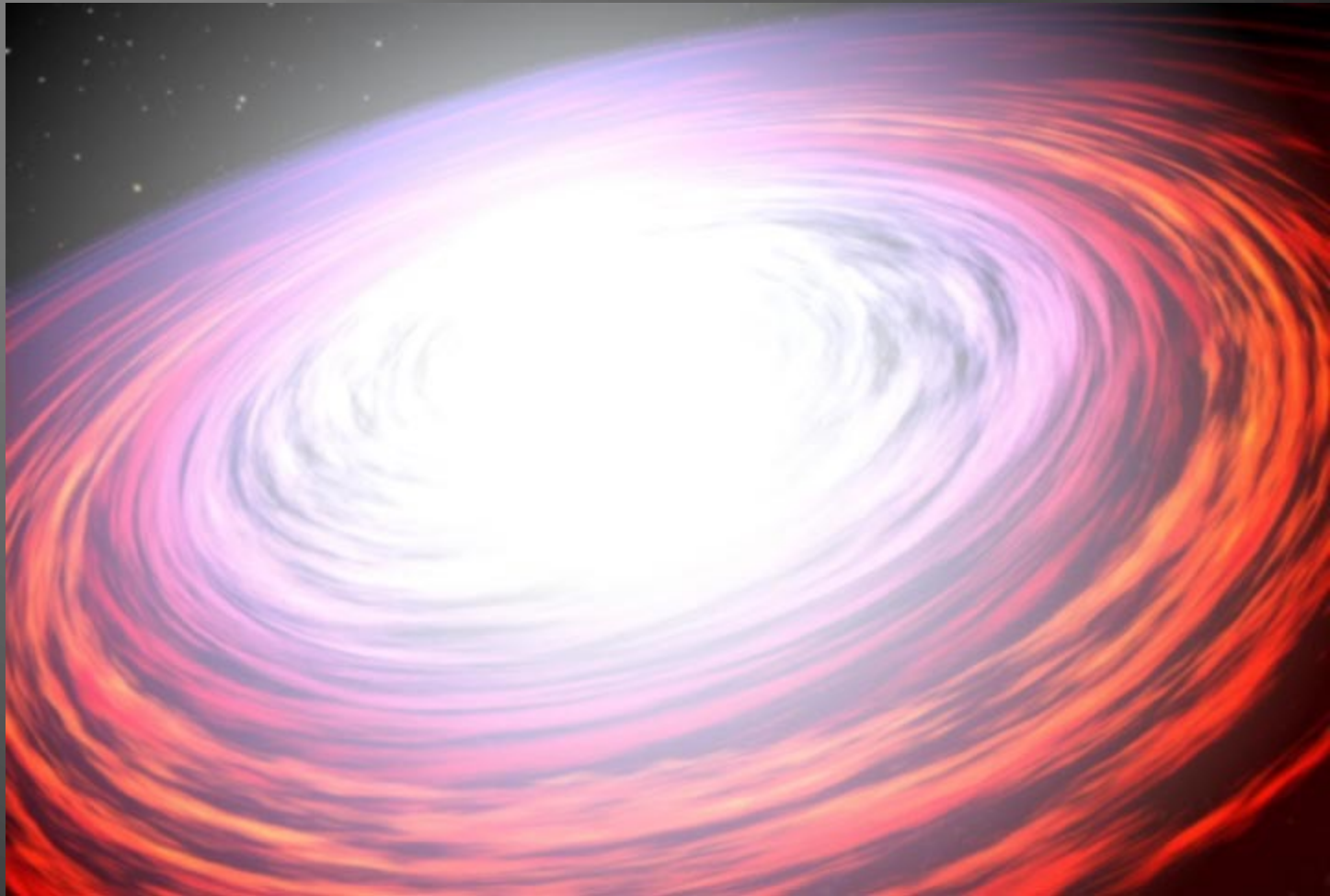
From Stars to
X-ray Binaries and
Gravitational Wave Sources

PRINCETON SERIES IN ASTROPHYSICS

THE ACCRETING NEUTRON STAR



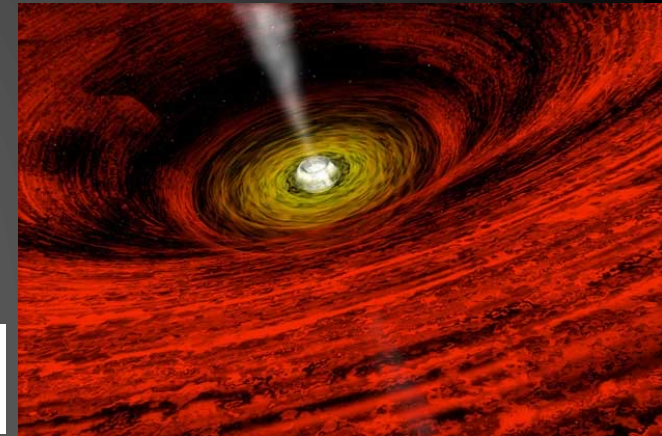
Energetics of accretion





Released gravitational binding energy (infall from ∞)

$$\Delta U = \frac{GMm}{R}$$



$1M_{\odot}$ accretor and $L_x = 10^{37} \text{ erg s}^{-1}$

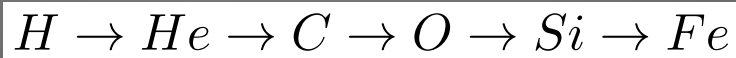
Stellar object	Radius (km)	$\Delta U/mc^2$	$\Delta U/m$ (erg g $^{-1}$)	dM/dt ($M_{\odot} \text{ yr}^{-1}$)	Column density (g cm $^{-2}$)
Sun	7×10^5	2×10^{-6}	2×10^{15}	1×10^{-4}	140
White dwarf	10000	2×10^{-4}	1×10^{17}	1×10^{-6}	16
Neutron star	10	0.15	1×10^{20}	1×10^{-9}	0.5
Black hole	3	0.1-0.4	4×10^{20}	4×10^{-10}	0.3

Note: X-rays are stopped at column densities larger than a few g cm $^{-2}$

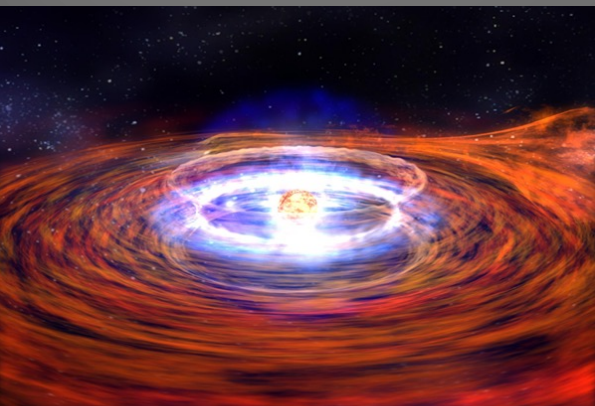
Accretion Luminosity

$$L_X = (\varepsilon_{nuc} + \varepsilon_{grav}) \dot{M}_{acc}$$

Nuclear burning at surface of compact object

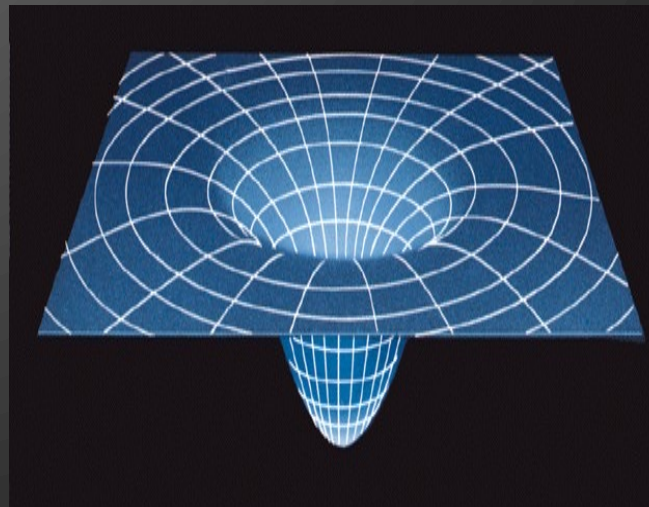
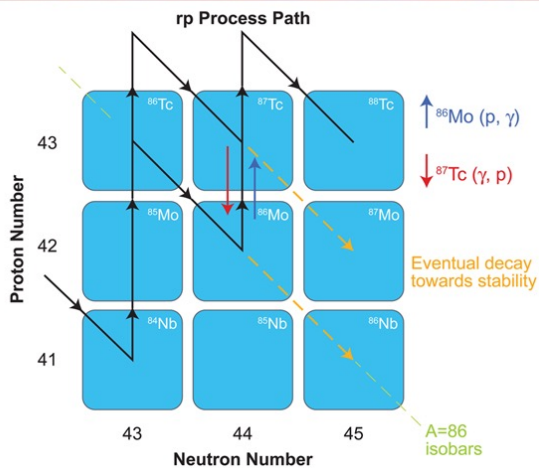


Dominate in accreting WD
(not relevant for BH)



Dominate in NS and BH

Release of gravitational binding energy



Accretion-, rotation-, thermal-, and magnetic field-powered X-ray sources

❖ Accretion-powered X-ray sources

- Accretion of material from a companion star
 - ✓ white dwarf (CV, classical/dwarf novae, AM CVn, super-soft X-ray sources)
 - ✓ neutron star regular pulsed emission (HMXB)
 - ✓ neutron star X-ray burst sources (LMXB)
 - ✓ black hole soft X-ray transients (SXT)
 - ✓ continuous emission from hot accretion disks

Binaries

❖ Rotation-powered X-ray sources

Isolated NS

- Crab pulsar, Geminga etc. (non-accreting X-ray pulsar)

❖ Thermal-powered X-ray sources

- Continuous black body radiation from hot young neutron stars (XDINs)

❖ Magnetic-field powered X-ray sources

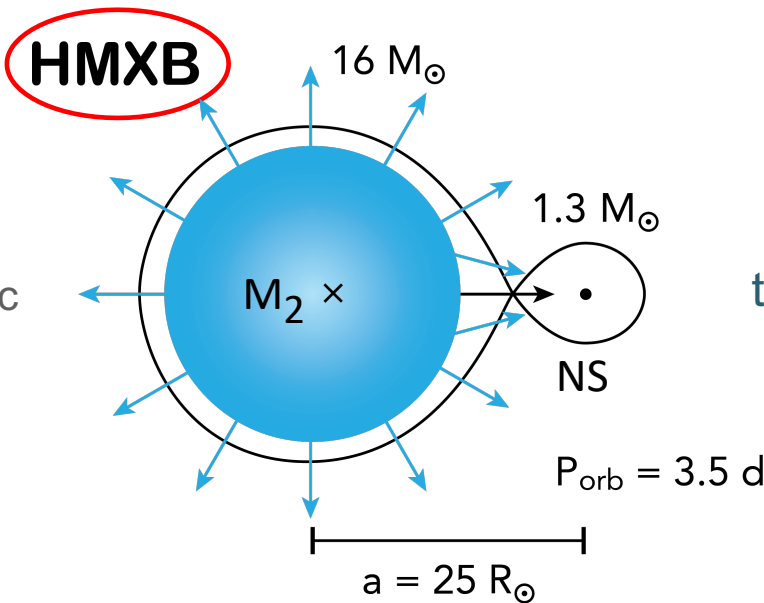
- Magnetars (SGRs and AXPs)



High-Mass X-ray Binaries



- wind accretion
- beginning atmospheric Roche-lobe overflow



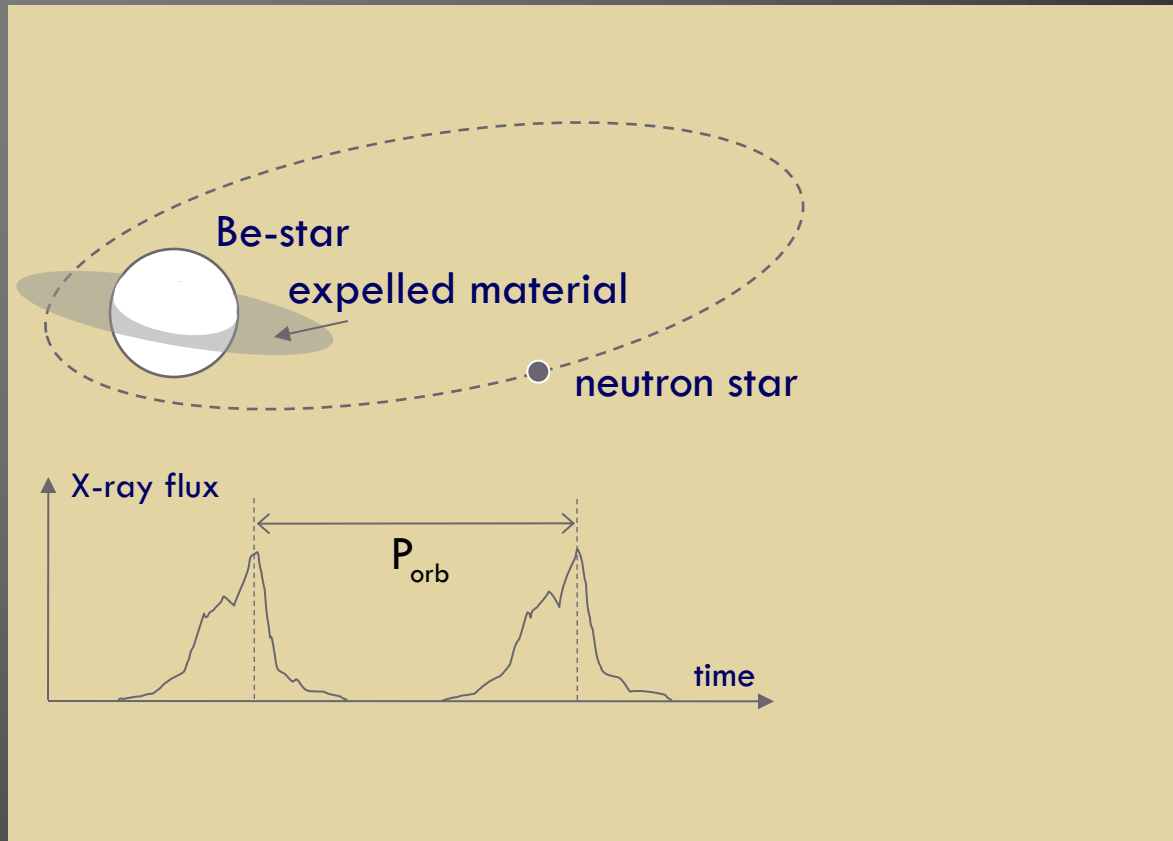
timescale: $10^5 - 10^6$ yr

Donor star masses $M_2 > 10 M_{\odot}$. NS or BH accretors.

114 systems known in our Galaxy:

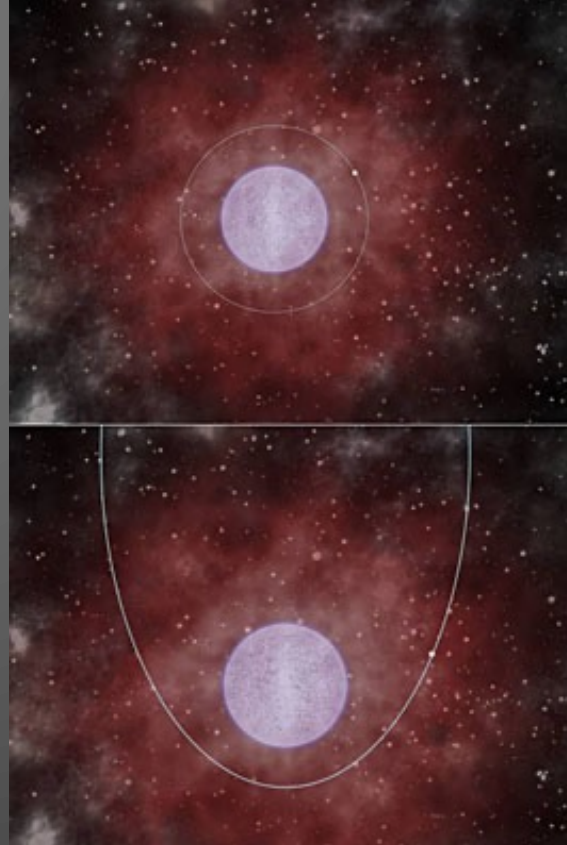
- 50 systems with measured $P_{\text{orb}} = 0.2 - 262$ days (median 23 days)
- 66 systems with measured $P_{\text{spin}} = 33 \text{ ms} - 4 \text{ hours}$ (median 3 min)

Be-star X-ray binary



Supergiant Fast X-ray Transients (SFXTs)

(subclass of HMXBs – many discovered with INTEGRAL)



HMXBs with BH accretors

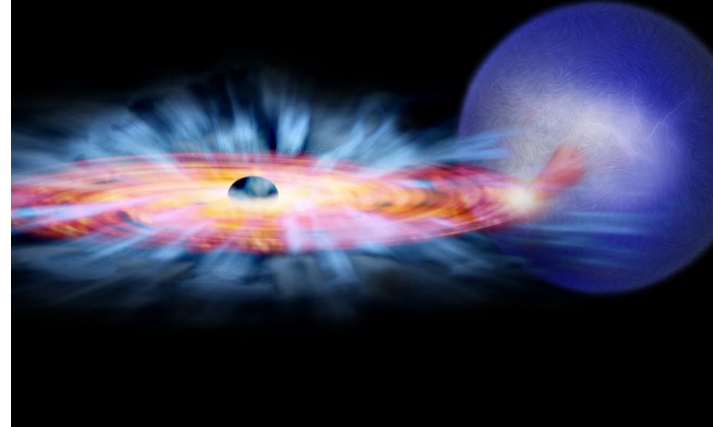


Table 6.6: The five known BH HMXBs. (Updated after van den Heuvel, 2019).

Source	P_{orb} (d)	M_{donor} (M_{\odot})	M_{BH} (M_{\odot})	Reference
Cyg X-1	5.6	41 (± 7)	21.2 (± 2.2)	Miller-Jones et al. (2021)
LMC X-1	3.9	31.8 (± 3.5)	10.9 (± 1.4)	Orosz et al. (2009)
LMC X-3	1.7	3.6 (± 0.6)	7.0 (± 0.6)	Orosz et al. (2014)
MCW 656	~ 60	~ 13	4.7 (± 0.9)	Casares et al. (2014)
M33 X-7	3.45	70 (± 7)	15.7 (± 1.5)	Orosz et al. (2007)

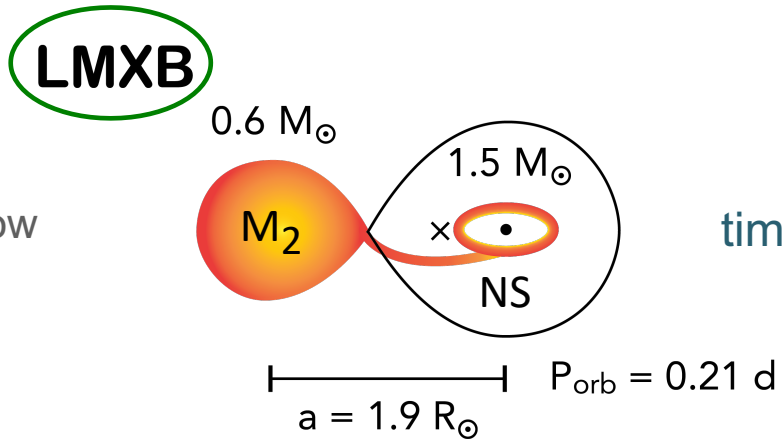
Tauris & van den Heuvel (2023)



Low-Mass X-ray Binaries



- Roche-lobe overflow



timescale: $10^8 - 10^9 \text{ yr}$

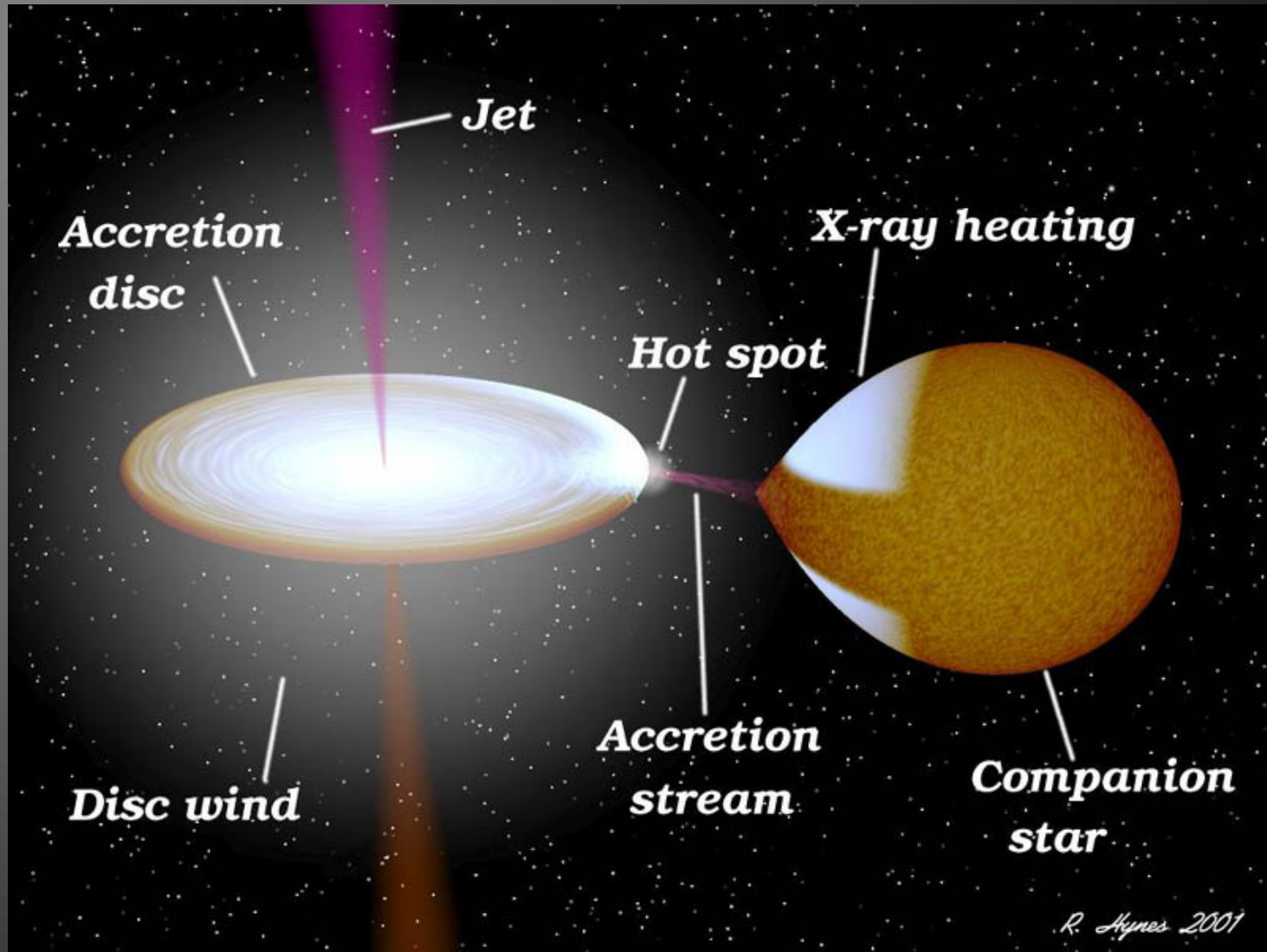
Donor star masses $M_2 < 1 M_{\text{sun}}$. NS or BH accretors.

187 candidate systems in our Galaxy:

- 74 systems with measured $P_{\text{orb}} = 11 \text{ min} - 1160 \text{ days}$ (median: 8 hours)
- 26 systems with measured $P_{\text{spin}} = 1.6 \text{ ms} - 7.7 \text{ sec}$ (median: 3 ms)

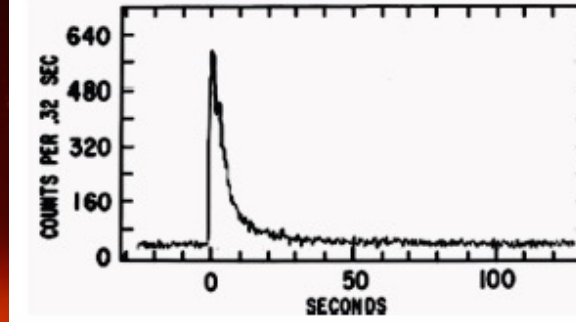
Most systems are **transients** and **X-ray bursters** (thermonuclear explosions)

About 20 **black hole** systems (**soft X-ray transients**)



X-ray bursts

Burst light curve



Rise time $\approx 0.5 - 5$ seconds
Decay time $\approx 10 - 100$ seconds
Recurrence time \approx hours to day
Energy release $\approx 10^{39}$ erg

Accretion of H-rich matter piles up on the NS.
Gravity compresses matter and the temperature rises at the base of this accumulated envelope leading to ignition under degenerate conditions resulting in a thermonuclear explosion and a rapid photospheric expansion.
The burst lasts for some 10-100 sec.
Burst oscillations reveal the spin period of the NS.

HARDY

Equipotential surfaces

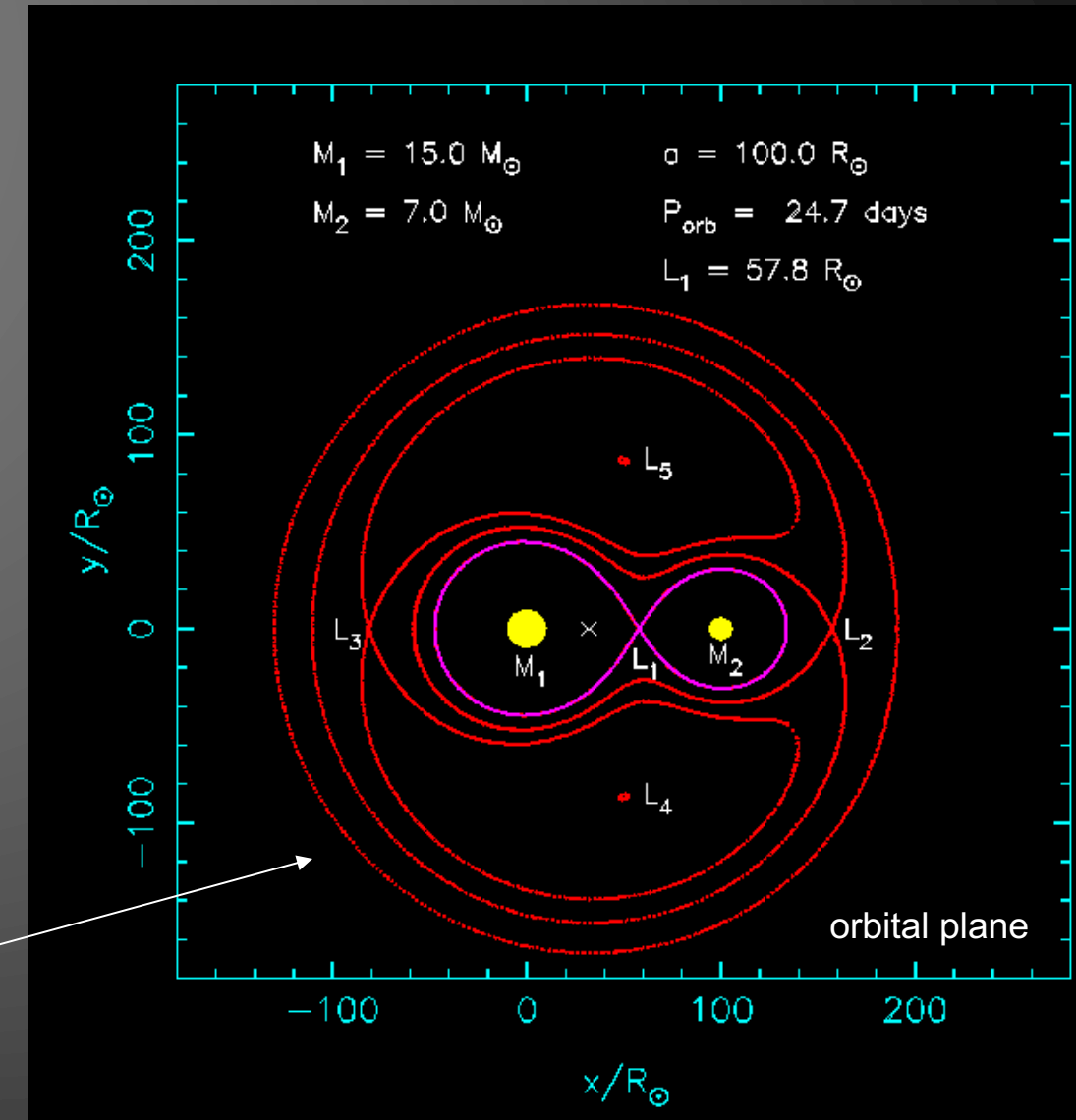
Effective gravitational potential:

$$\Phi = -\frac{GM_1}{r_1} - \frac{GM_2}{r_2} - \frac{\Omega^2 r_3^2}{2}$$

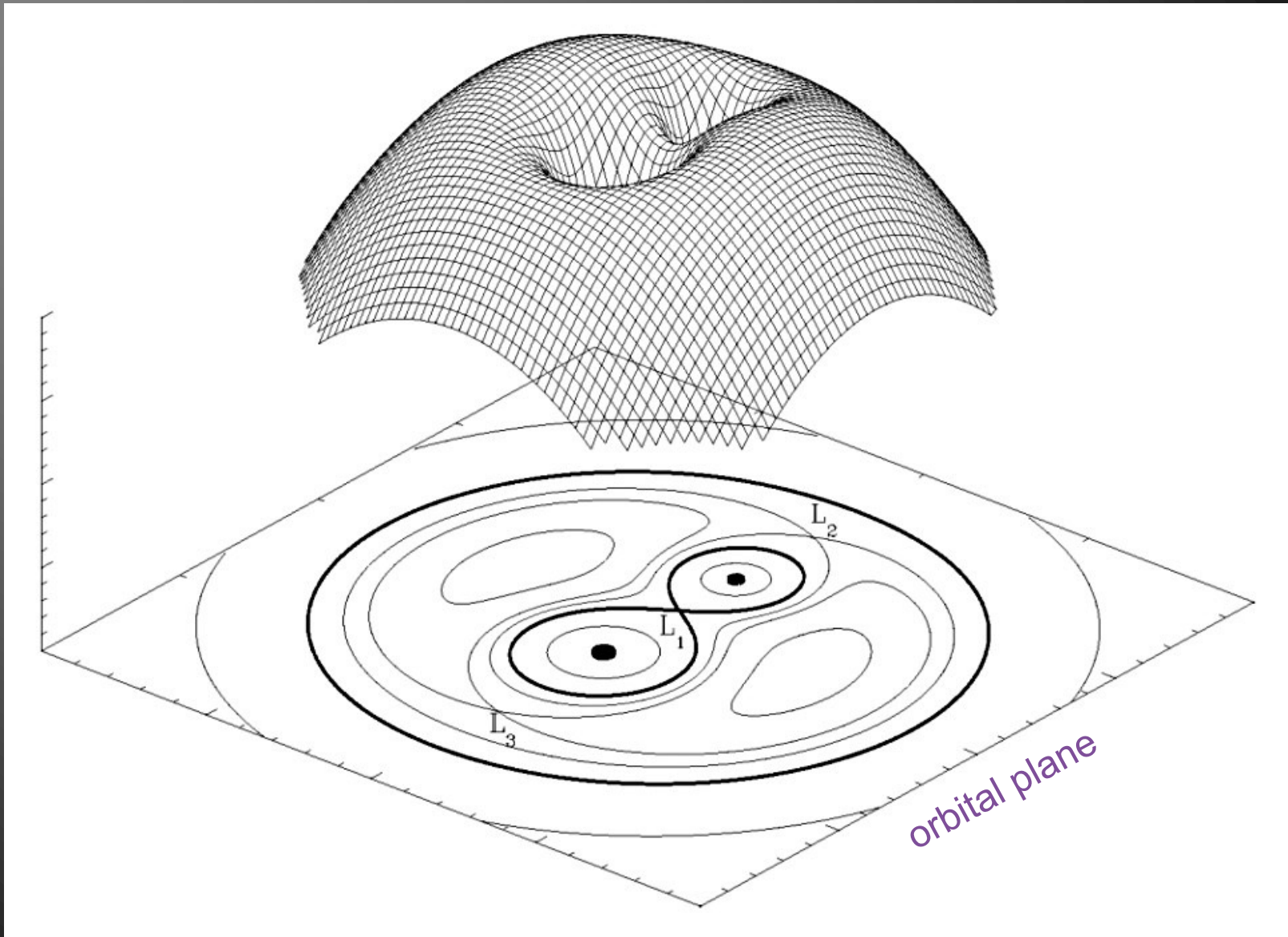
Roche-lobe radius:

$$\frac{R_L}{a} = \frac{0.49 q^{2/3}}{0.6 q^{2/3} + \ln(1 + q^{1/3})}$$

co-moving frame



Equipotential surfaces



X-ray binaries Roche-lobe overflow Cases A, B and C: (the evolutionary stage of the donor star at onset of RLO is quite important ...)

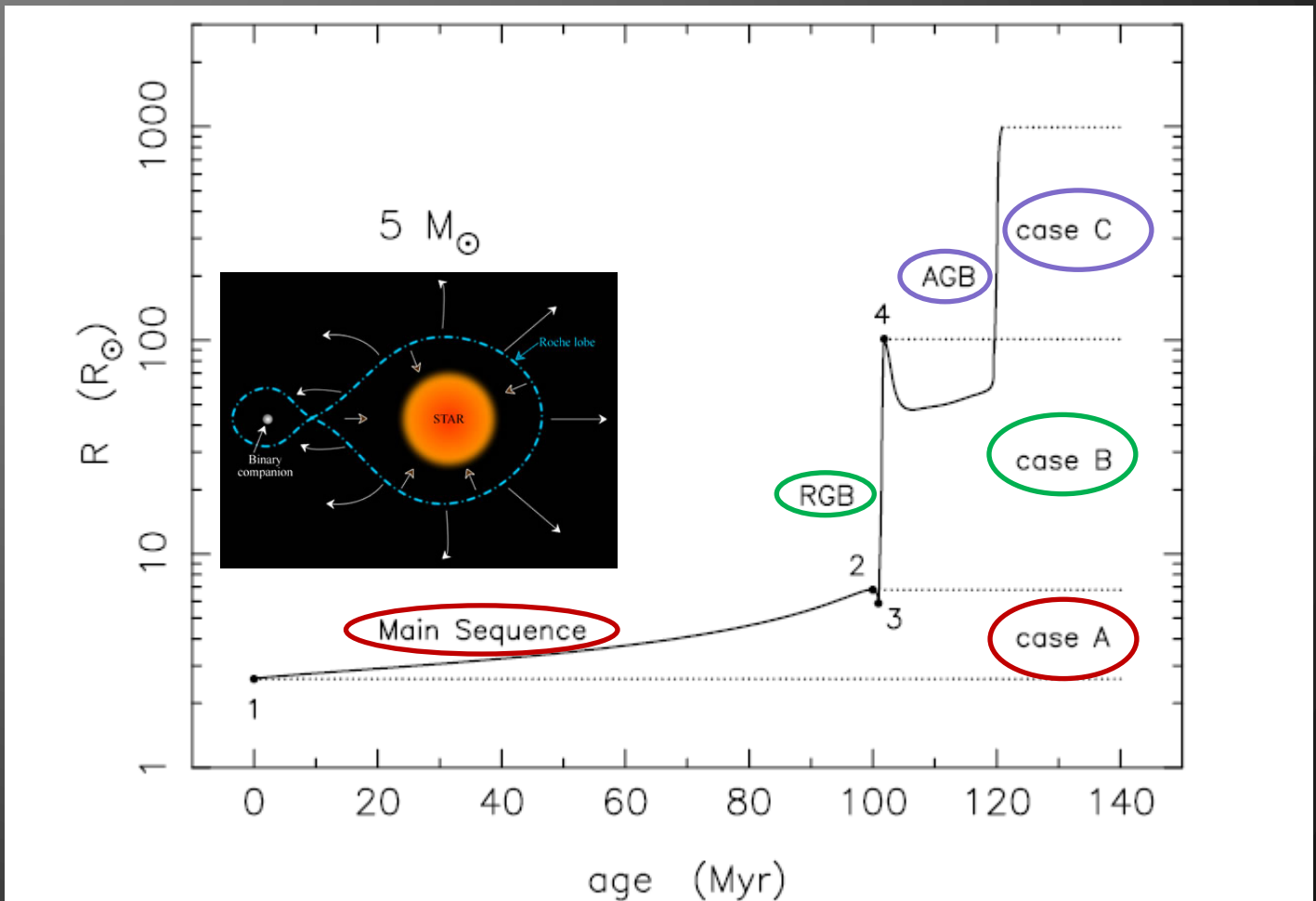


Fig. 16.6. Evolutionary change of the radius of the $5 M_{\odot}$ star plotted in Fig. 16.5. The ranges of radii for mass transfer to a companion star in a binary system according to RLO cases A, B and C are indicated – see Section 16.4 for an explanation.

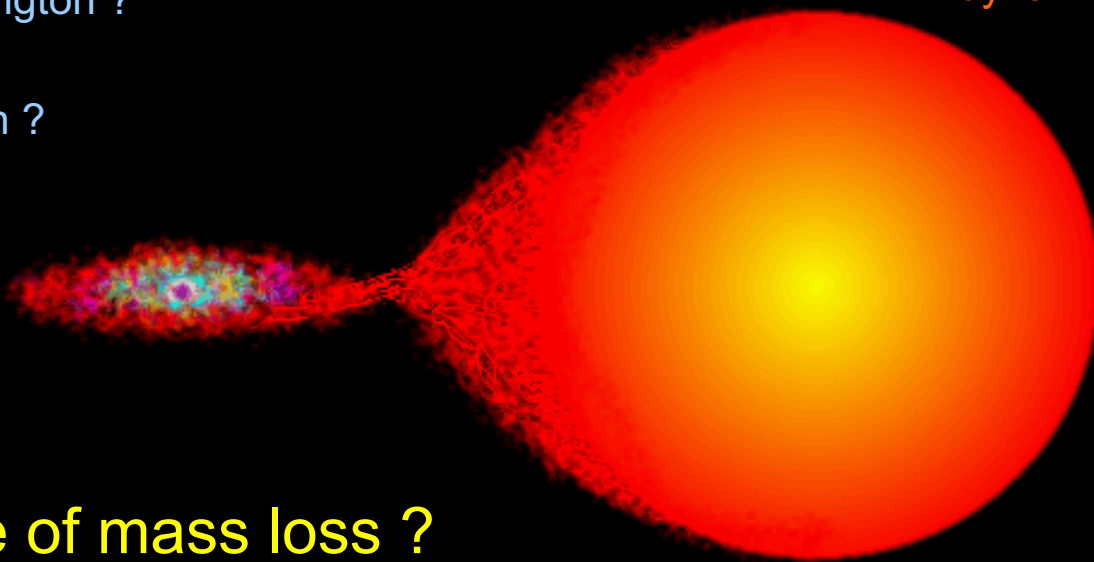
The evolution of compact binaries

Accretion ?

super-Eddington ?

jet ?

B-field, spin ?



Mode of mass loss ?

specific orbital angular momentum ?

magnetic braking / tidal interactions

gravitational wave radiation

Stability ?

response of donor star ?

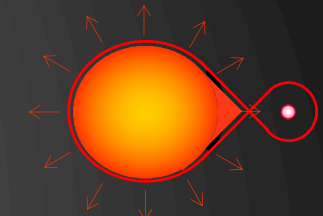
response of Roche-lobe ?

dynamically stable ?

Stability criteria for mass transfer

exponents of radius to mass: $R \propto M^\zeta$

$$\zeta_{\text{donor}} \equiv \frac{\partial \ln R_2}{\partial \ln M_2} \quad \wedge \quad \zeta_L \equiv \frac{\partial \ln R_L}{\partial \ln M_2}$$



response of the Roche lobe to mass loss

adiabatic or thermal response of the donor star to mass loss

initial stability criteria: $\zeta_L \leq \zeta_{\text{donor}}$

Change in stellar radius:

$$\dot{R}_2 = \frac{\partial R_2}{\partial t} \Big|_{M_2} + R_2 \zeta_{\text{donor}} \frac{\dot{M}_2}{M_2}$$

nuclear burning

Change in Roche-lobe radius:

$$\dot{R}_L = \frac{\partial R_L}{\partial t} \Big|_{M_2} + R_L \zeta_L \frac{\dot{M}_2}{M_2}$$

tidal spin-orbit couplings
gravitational wave radiation

$\dot{R}_2 = \dot{R}_L$ yields mass-transfer rate!

Stability criteria for mass transfer II

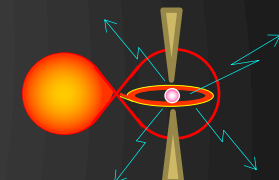
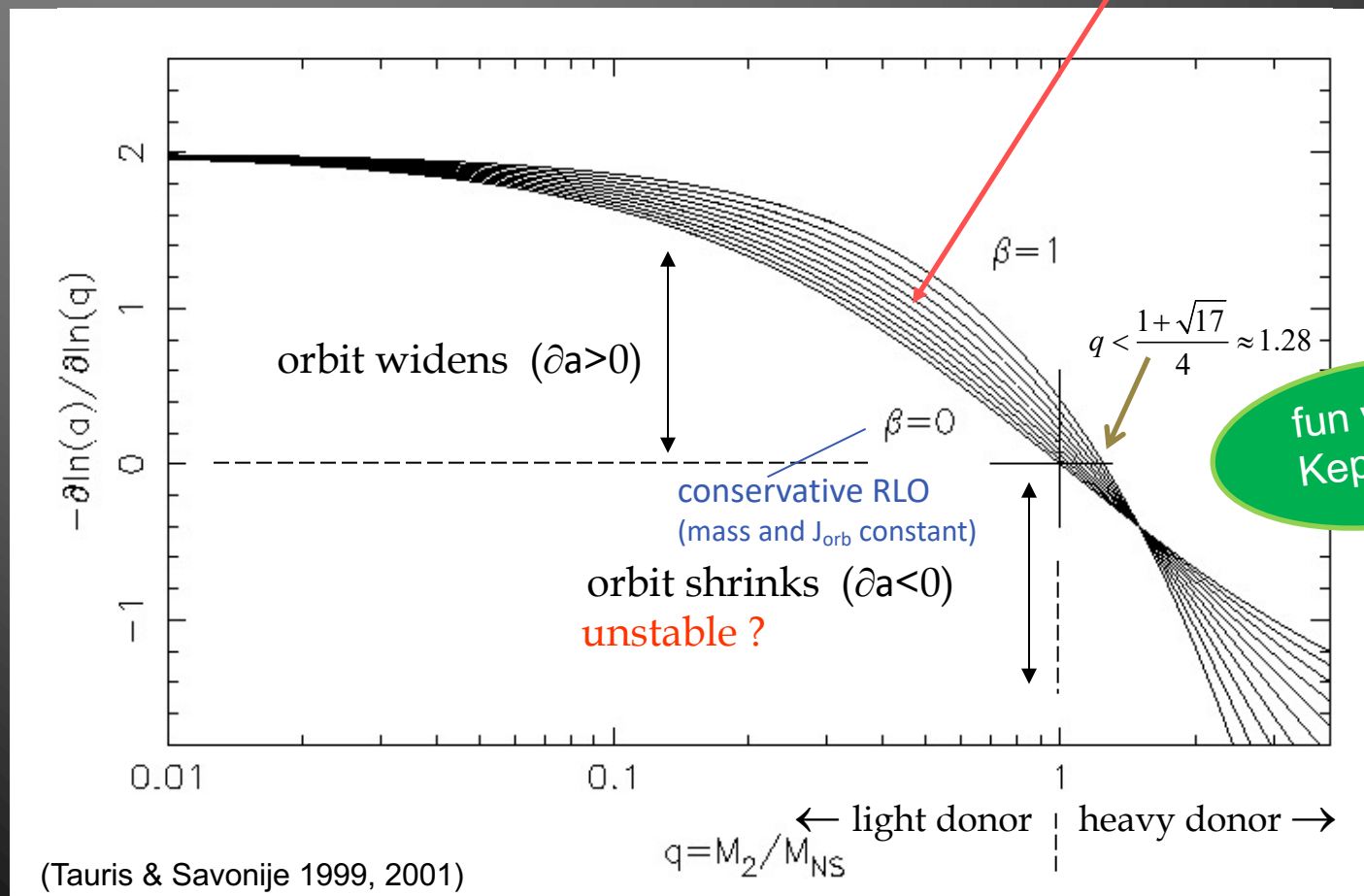
orbital separation, a
mass ratio, q

- Isotropic re-emission model

Orbital evolution:

$$-\frac{\partial \ln a}{\partial \ln q} \quad \wedge \quad q = \frac{M_2}{M_{NS}} \quad (\partial q < 0)$$

$$\beta = \max\left(\frac{|\dot{M}_2| - \dot{M}_{Edd}}{|\dot{M}_2|}, 0\right) \quad \alpha = 0 \quad \delta = 0$$



Summary

- Lighter donor: orbit widens
- Heavier donor: orbit shrinks

The Orbital Angular Momentum Balance Equation

$$J_{orb} = \frac{M_1 M_2}{M} \Omega a^2 \sqrt{1 - e^2}$$

orbital angular momentum

logarithmic differentiation
 \Downarrow (e=0, tidal circularization)

$$\frac{\dot{a}}{a} = 2 \frac{\dot{J}_{orb}}{J_{orb}} - 2 \frac{\dot{M}_1}{M_1} - 2 \frac{\dot{M}_2}{M_2} + \frac{\dot{M}_1 + \dot{M}_2}{M}$$

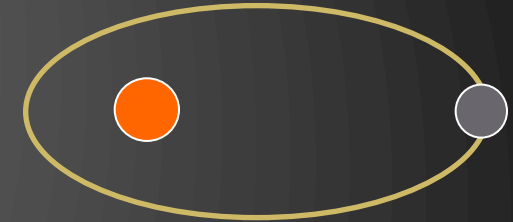
$$J_{orb} = |\vec{r} \times \vec{p}|$$

$$\Omega = \sqrt{GM / a^3}$$

$$\frac{\dot{J}_{orb}}{J_{orb}} = \frac{\dot{J}_{gwr}}{J_{orb}} + \frac{\dot{J}_{mb}}{J_{orb}} + \frac{\dot{J}_{ls}}{J_{orb}} + \frac{\dot{J}_{ml}}{J_{orb}}$$

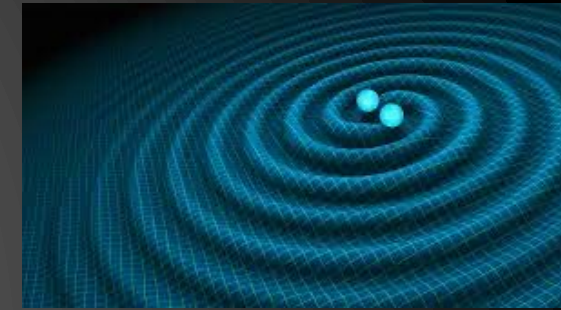
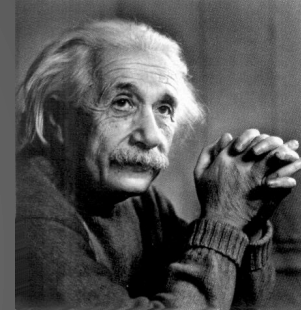
GW radiation magnetic braking (other) spin-orbit couplings mass loss

see the next slides...



Gravitational wave radiation:

$$\frac{\dot{J}_{gwr}}{J_{orb}} = - \frac{32}{5} \frac{G^3}{c^5} \frac{M_1 M_2 M}{a^4}$$



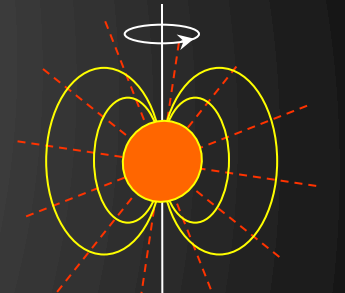
Magnetic braking:

$$\frac{\dot{J}_{mb}}{J_{orb}} \propto - \frac{k^2 R^4}{a^5} \frac{GM^3}{M_1 M_2}$$

(uncertain)

Low-mass stars: magnetic wind!
⇒ loss of spin angular momentum

In tight binaries the system
is tidally locked (synchronized)
and spin-orbit couplings operate
⇒ loss of orbital angular momentum



$M_2 < 1.5 M_{\text{sun}}$

$P_{\text{orb}} < 2 \text{ days}$

Spin-orbit couplings:

$$\frac{\dot{J}_{ls}}{J_{orb}}$$

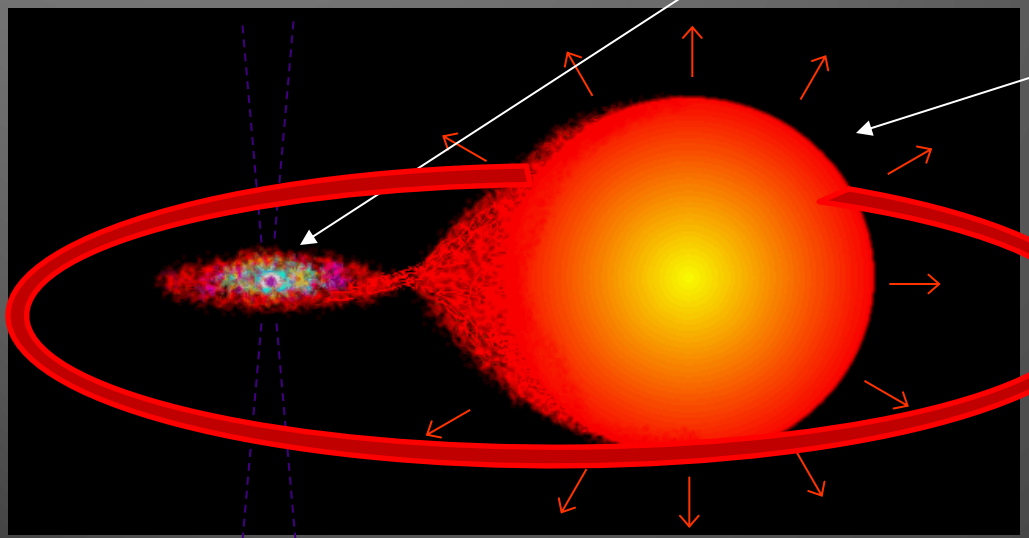
- fx . change in stellar moment of inertia
(as a result of nuclear burning or mass loss)

Isotropic re-emission model:

$$\frac{\dot{J}_{ml}}{\dot{J}_{orb}} = \frac{\alpha + \beta q^2 + \delta \gamma (1+q)^2}{1+q} \frac{\dot{M}_2}{\dot{M}_2}$$

$$\beta = \max \left(\frac{|\dot{M}_2| - \dot{M}_{Edd}}{|\dot{M}_2|}, 0 \right)$$

β : mass ejected from accretor
 - fx. in a relativistic jet
 (isotropic re-emission)



α : loss in a direct fast wind

δ : mass loss via circumbinary
 coplanar toroid with
 radius: $\gamma^2 a$

$0 \leq (\alpha, \beta, \delta) \leq 1$ fractions of the material transferred from donor to accretor

accretion efficiency: $\varepsilon = 1 - \alpha - \beta - \delta$ ($\partial M_{NS} = -\varepsilon \partial M_2$)

Solution....

Integration of the OAMB eq. for mass transfer/loss:

$$\frac{a}{a_0} = \Gamma_{ls} \left(\frac{q}{q_0} \right)^{2(\alpha+\gamma\delta-1)} \left(\frac{q+1}{q_0+1} \right)^{\frac{-\alpha-\beta+\delta}{1-\varepsilon}} \left(\frac{\varepsilon q + 1}{\varepsilon q_0 + 1} \right)^{3+2\frac{\alpha\varepsilon^2 + \beta + \gamma\delta(1-\varepsilon)^2}{\varepsilon(1-\varepsilon)}}$$

mass ratio

final separation (after RLO)

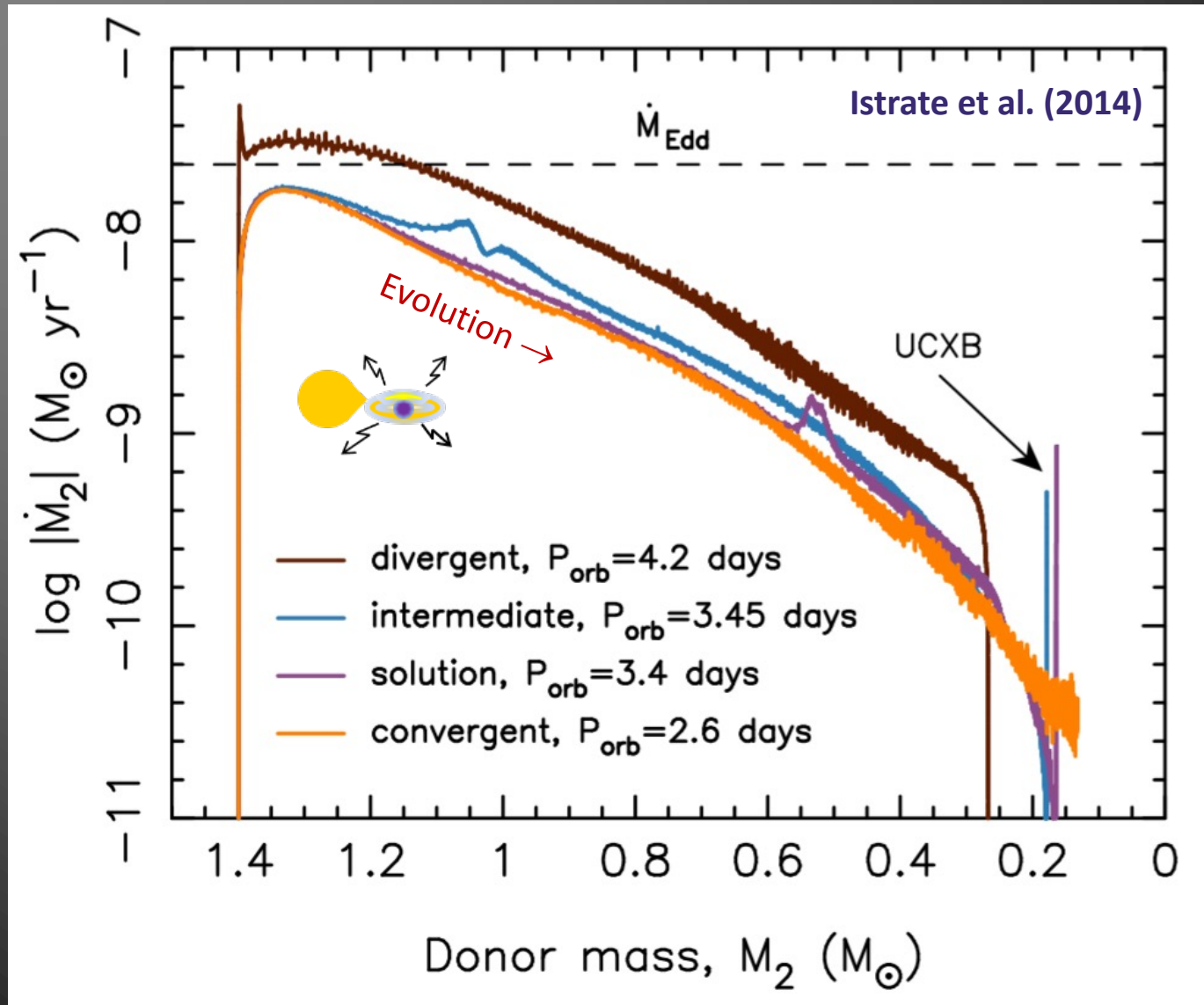
Tauris & van den Heuvel (2006)

Eq.(4.58) in Tauris & van den Heuvel (2023)

For simpler cases with direct wind mass loss or conservative RLO:

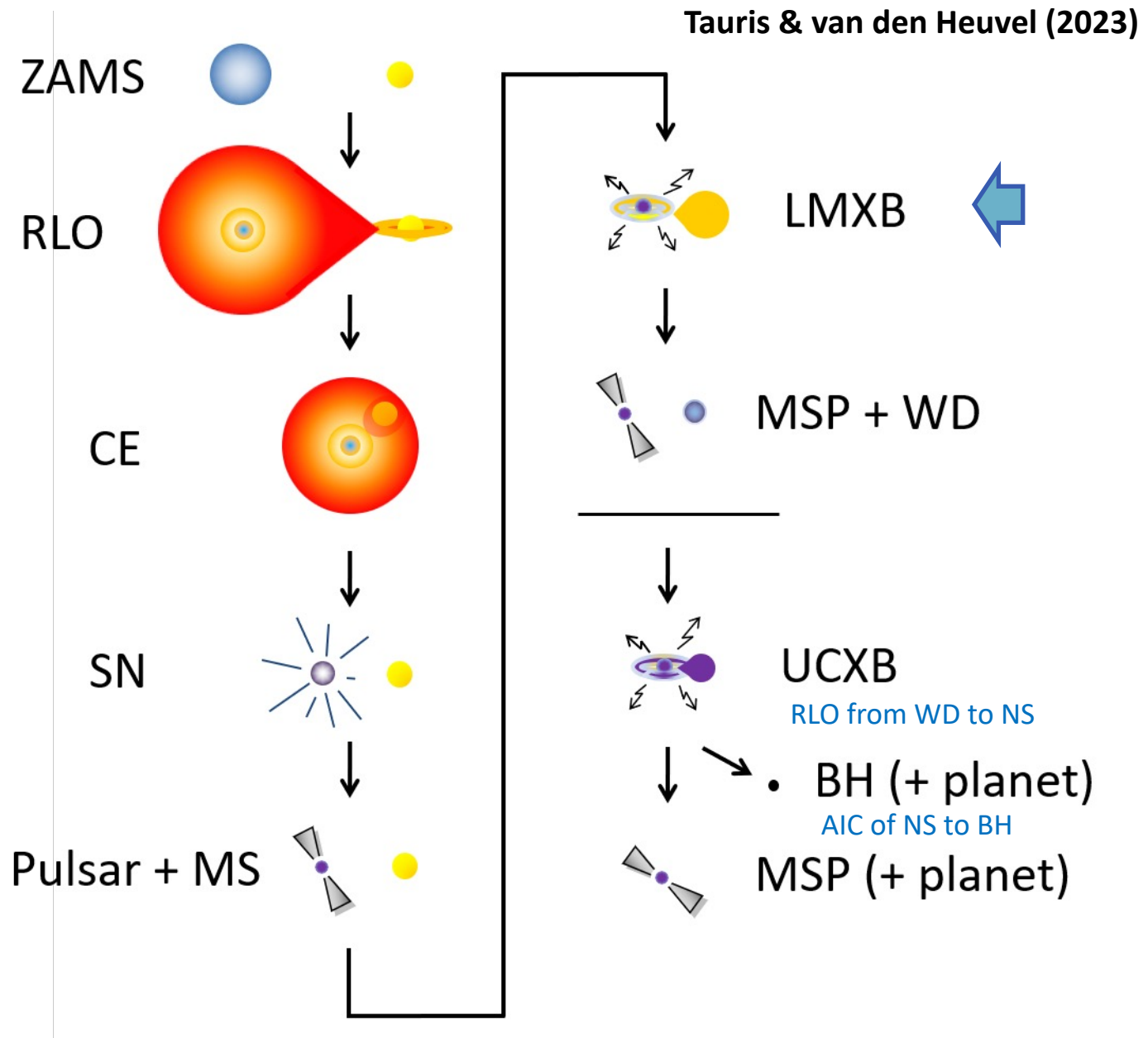
Ex.9+10

Example of numerical LMXB calculation.....



LMXB

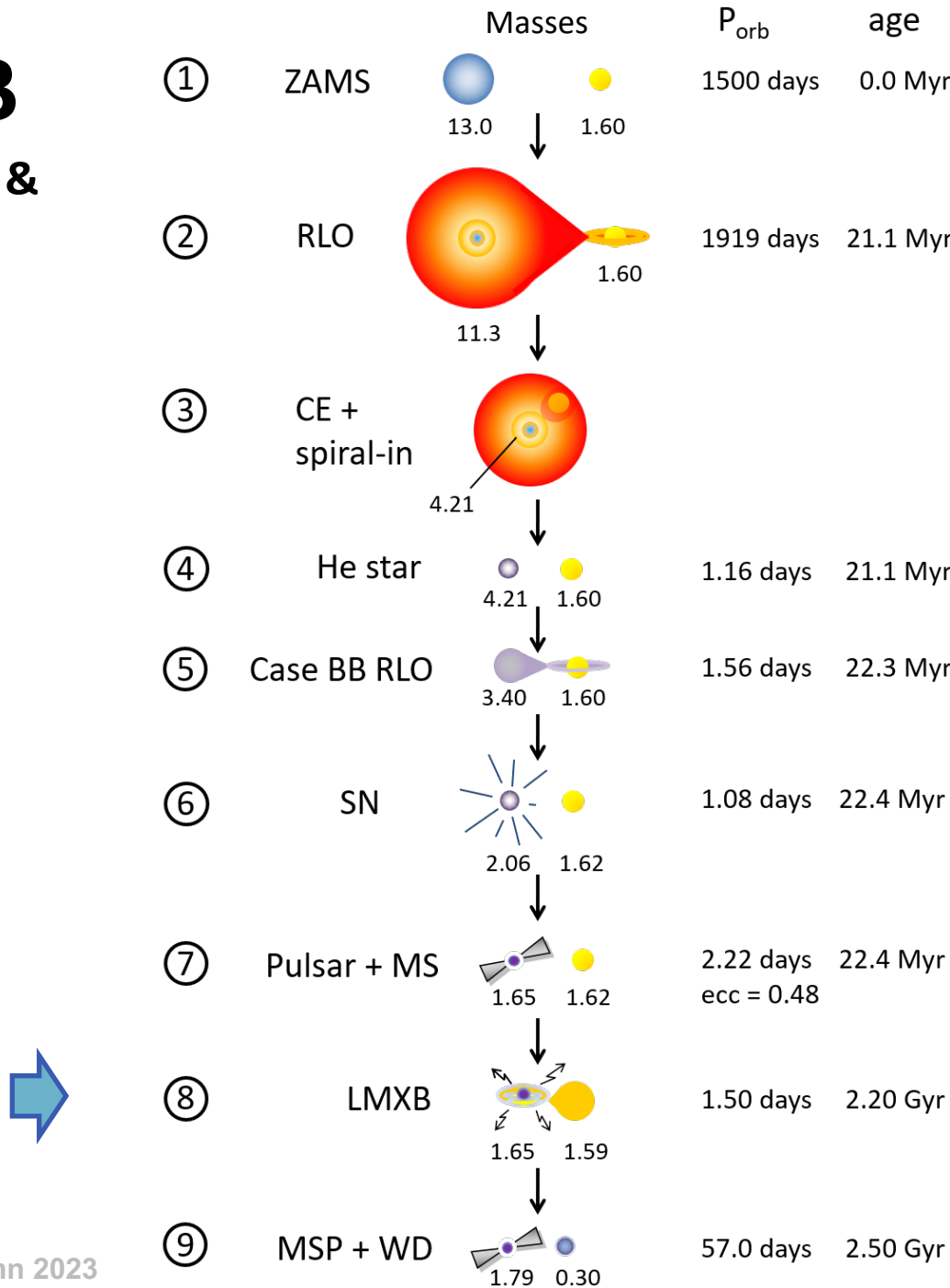
Formation & Evolution



LMXB

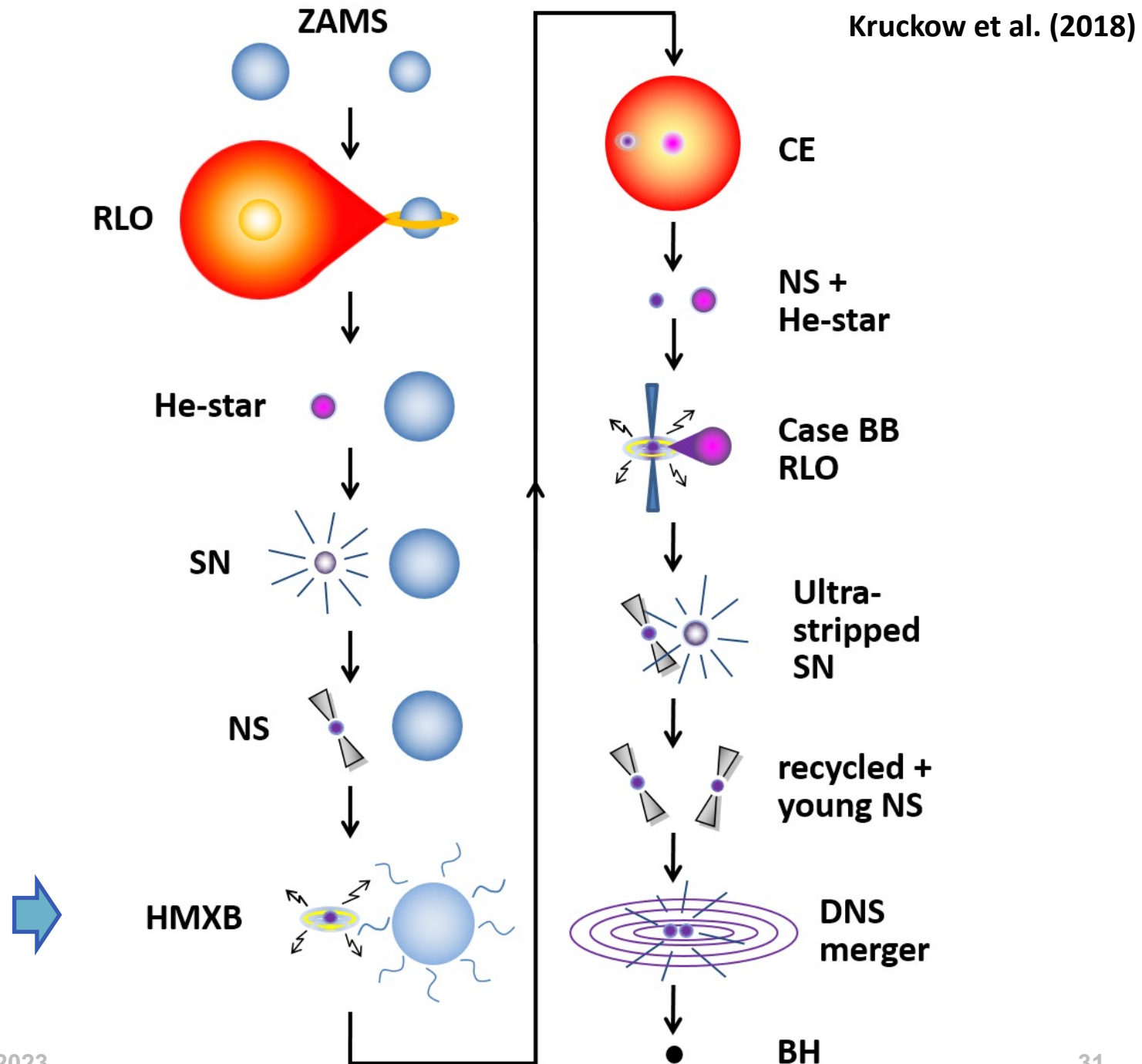
Formation & Evolution in detail

Tauris & van den Heuvel (2023)



HMXB

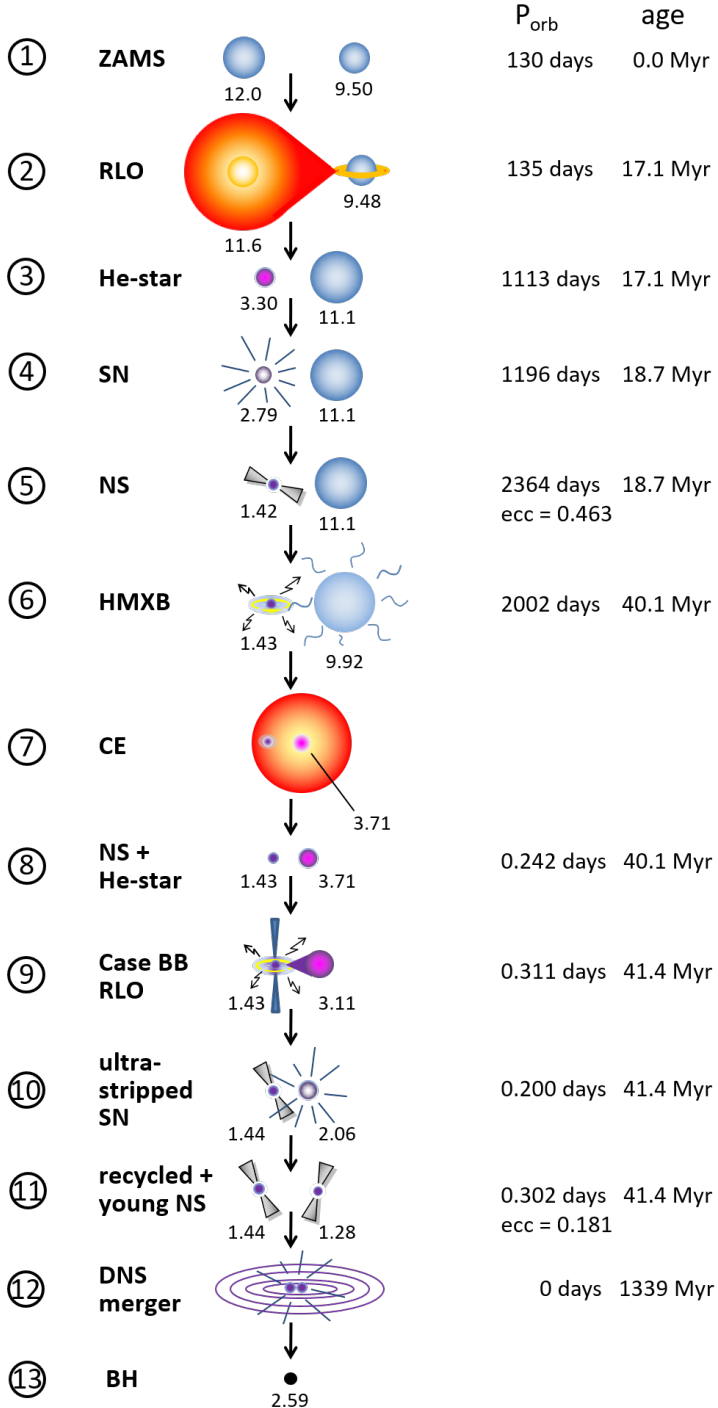
Formation & Evolution



Kruckow et al. (2018)

HMXB

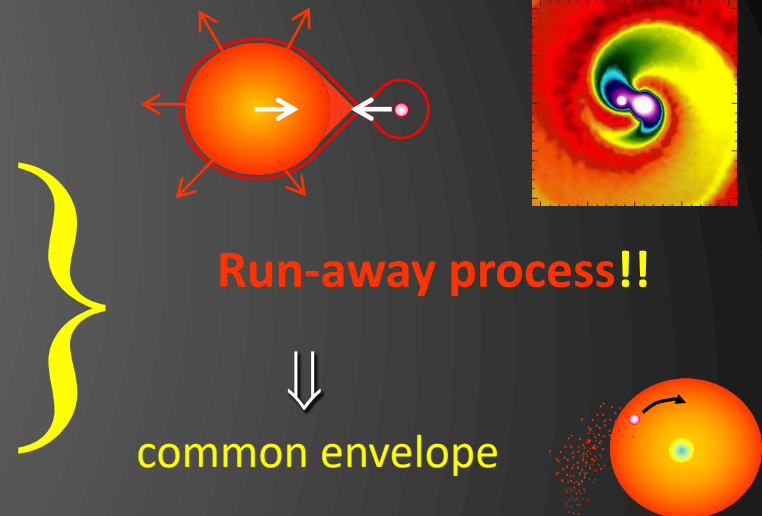
Formation & Evolution in detail



Common-Envelope + Spiral-in Evolution

Dynamically unstable mass transfer if:

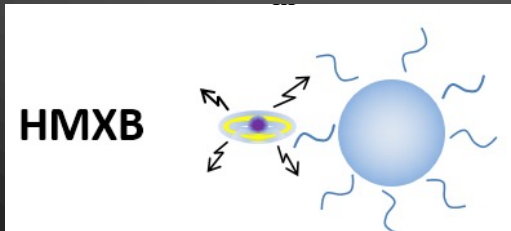
- deep convective envelope of donor star
= evolved giant star donors = wide orbits @ onset RLO
(b/c rapid expansion in response to mass loss)
- $M_{\text{donor}} > M_{\text{accretor}}$
(b/c orbit shrinks in response to mass loss)



drag force \rightarrow dissipation of orb. ang. mom. + deposition of E_{orb} in the envelope

Outcome HMXBs \rightarrow CE:

- CE: huge reduction of orbital separation



rejection of stellar envelope
(NS/BH orbiting a naked helium star)

merging of NS/BH + core
(Thorne-Zytkow object / BH)

COMMON-ENVELOPE EVOLUTION

$$\dot{E}_{orb} = -\frac{GM_{donor}M_{NS}}{2a^2} \frac{da}{dt} = \xi(\mu)\pi R_{acc}^2 \rho_{donor} v^3$$

Dissipation of E_{orb} by drag force (Bondi & Hoyle 1944)

$$E_{env} \equiv \alpha_{CE} \Delta E_{orb}$$

Webbink (1984)

$$\alpha_{CE} = 0.3 \sim 1$$

efficiency parameter

!

Energy of envelope:

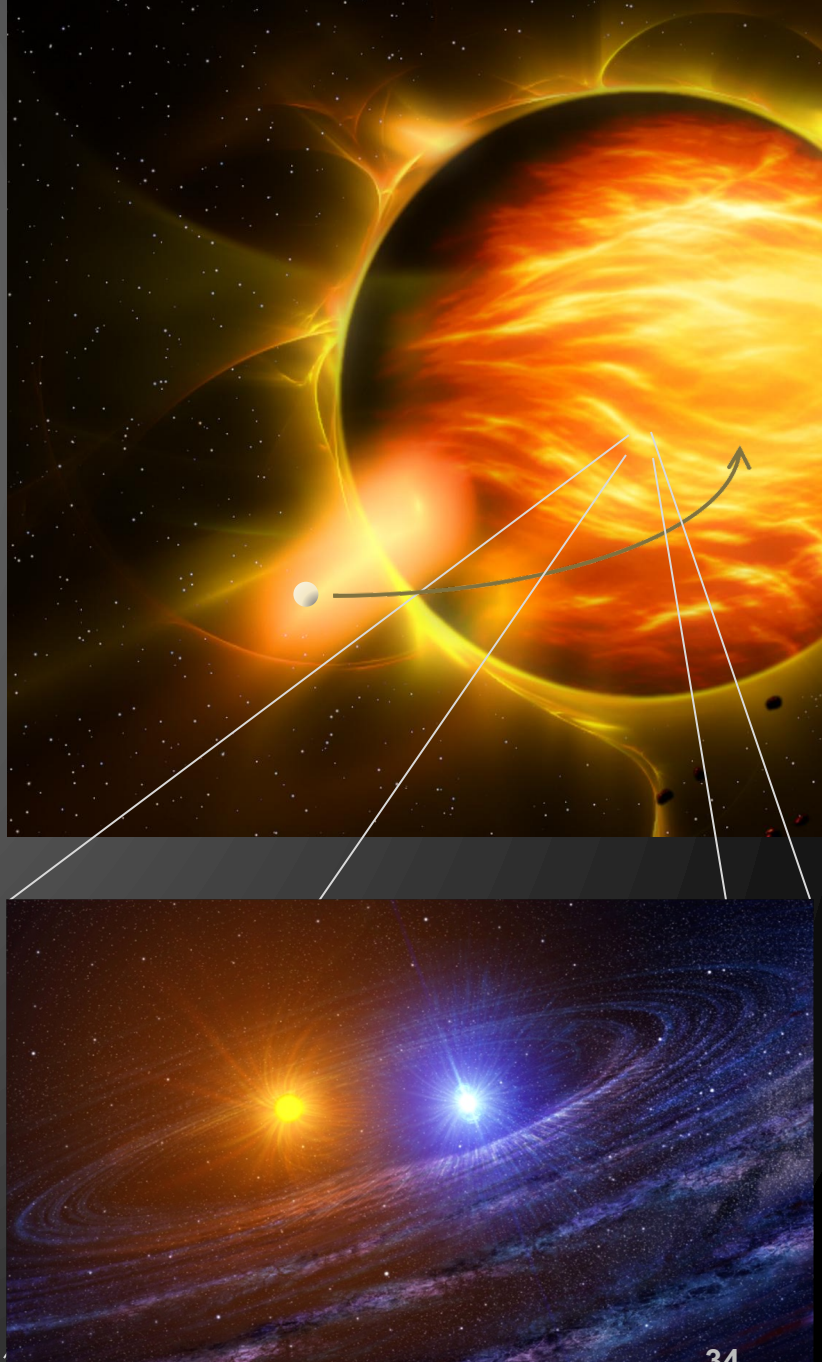
$$E_{env} = - \int_{M_{core}}^{M_{donor}} \frac{GM(r)}{r} dm + \alpha_{th} \int_{M_{core}}^{M_{donor}} U dm$$

gravitational binding energy

internal thermodynamic energy

Han et al. (1994, 1995)

- thermal energy
- energy of radiation
- ionization energy
- Fermi energy of e^- -gas



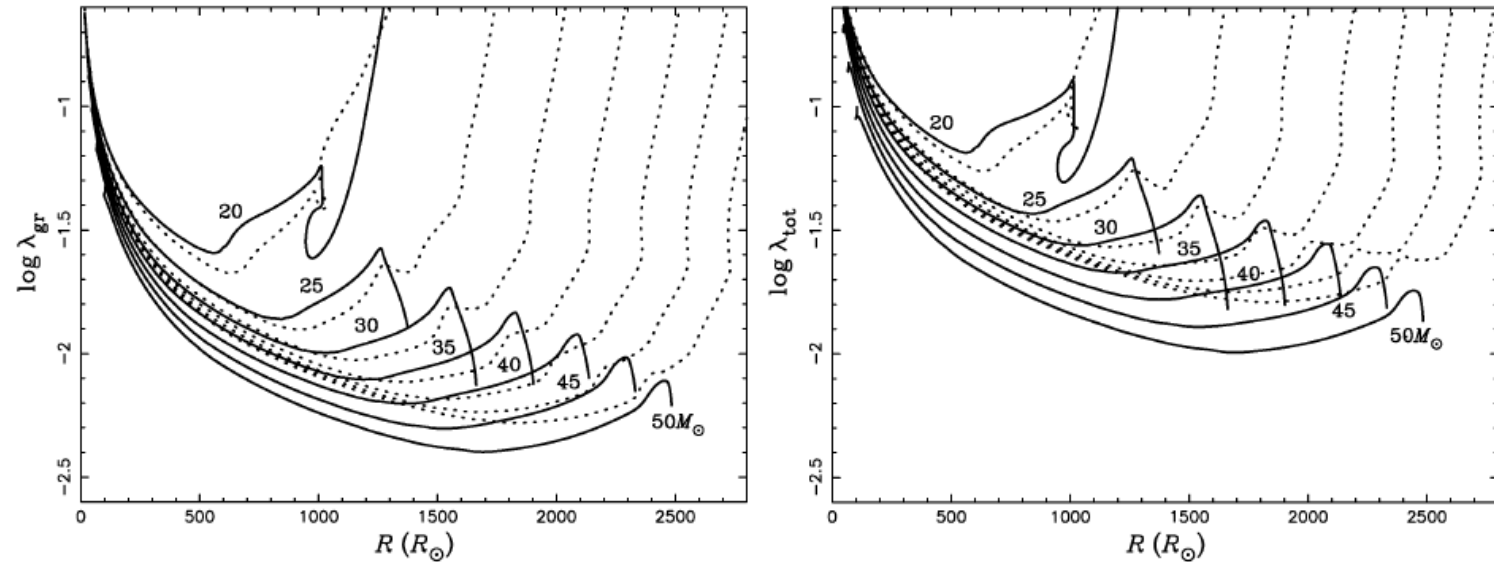


Figure 1. The envelope structure parameter λ as a function of stellar radius for different masses as indicated after hydrogen has been exhausted in the core. In the panels on the left, λ only includes the gravitational binding energy, while on the right λ includes both the gravitational binding energy and thermal energy (similar to Dewi & Tauris (2000)). The dotted curves are calculated without inclusion of a stellar wind. Note that in this case the dotted curves reach the largest radii attained by the models.

$$E_{env} \equiv -\frac{GM_{donor} M_{env}}{\lambda R_L}$$

de Kool (1990)

$$\lambda = 0.01 \sim 100$$

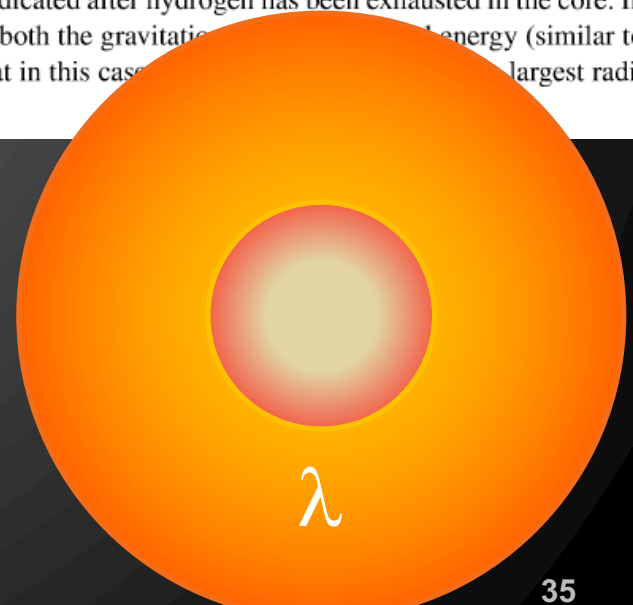
Dewi & Tauris (2000, 2001)

Podsiadlowski et al. (2003)

Xu & Li (2010)

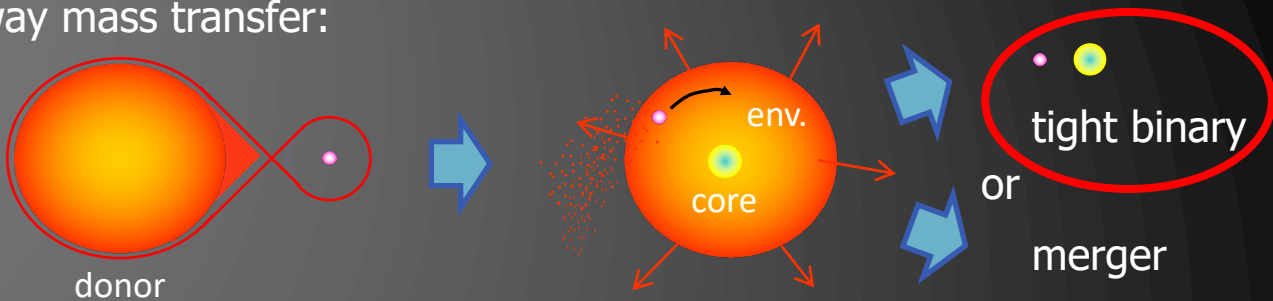
Loveridge et al. (2011)

Kruckow et al. (2016)



Common-Envelope + Spiral-in Evolution

Dynamically unstable run-away mass transfer:



$$E_{\text{env}} \equiv \alpha_{\text{CE}} \Delta E_{\text{orb}}$$

$$\alpha_{\text{CE}} = 0.3 \sim 1$$

$$E_{\text{env}} \equiv -\frac{GM_{\text{donor}} M_{\text{env}}}{\lambda R_L}$$

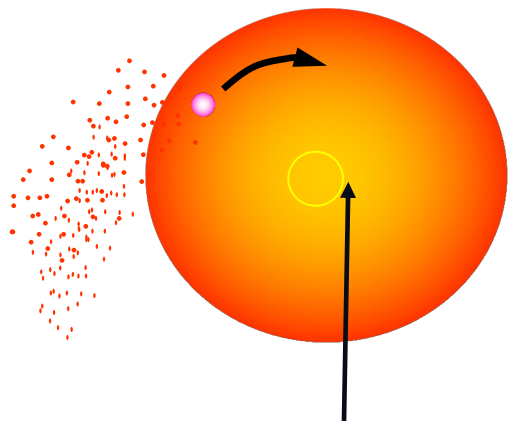
$$\Delta E_{\text{orb}} = -\frac{GM_{\text{core}} M_{\text{NS}}}{2a_f} + \frac{GM_{\text{donor}} M_{\text{NS}}}{2a_i}$$

$$\lambda = 0.01 \sim 100$$

$$\frac{a_f}{a_i} = \frac{M_{\text{core}} M_2}{M_{\text{donor}}} \frac{1}{M_2 + 2M_{\text{env}} / (\alpha_{\text{CE}} \lambda r_L)} \Rightarrow \frac{a_f}{a_i} \approx 10^{-3} - 10^{-2}$$

Ex. 11

COMMON ENVELOPE EJECTION



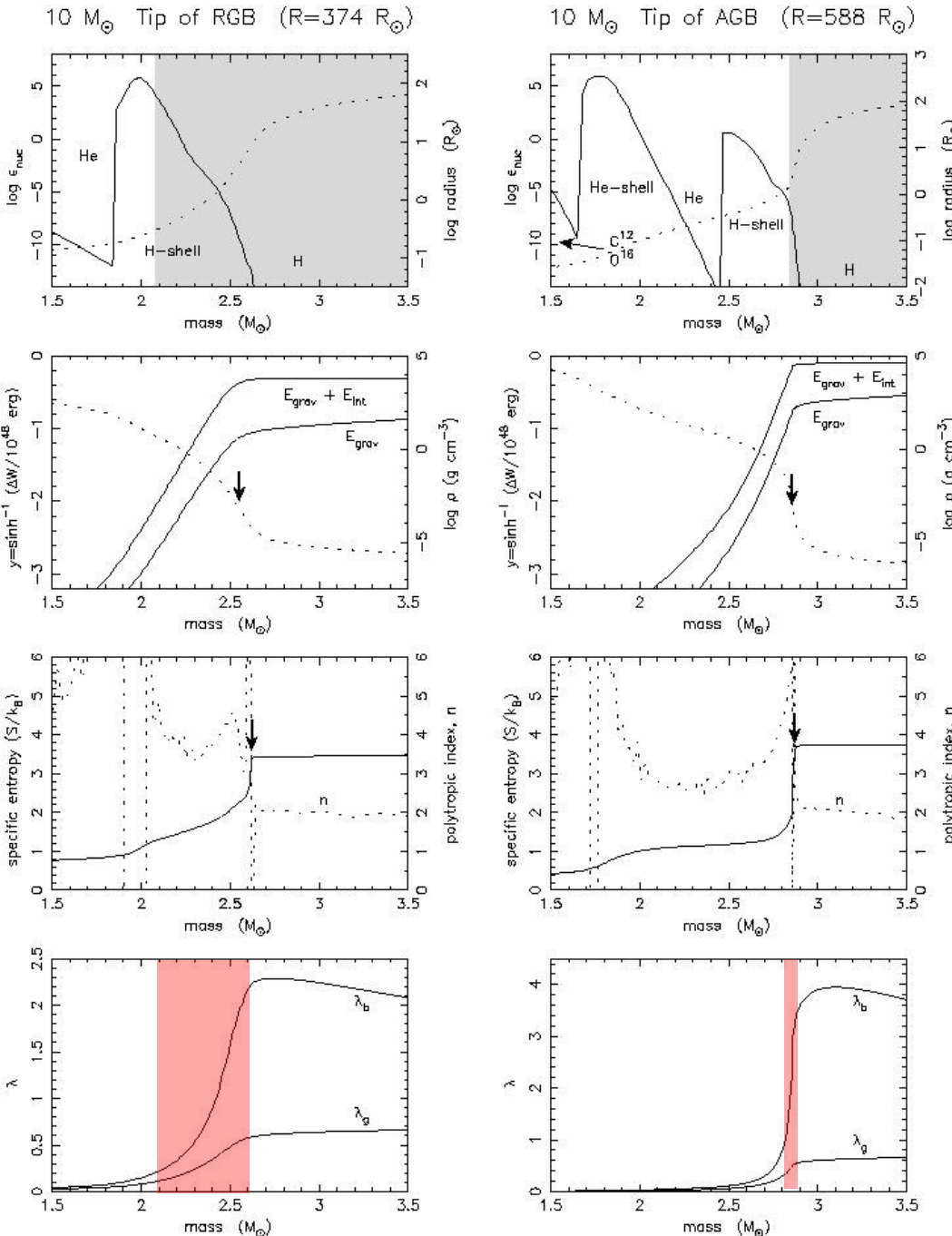
bifurcation point

Tauris & Dewi (2001)

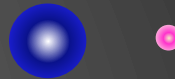
Ivanova (2011)

Kruckow et al. (2016)

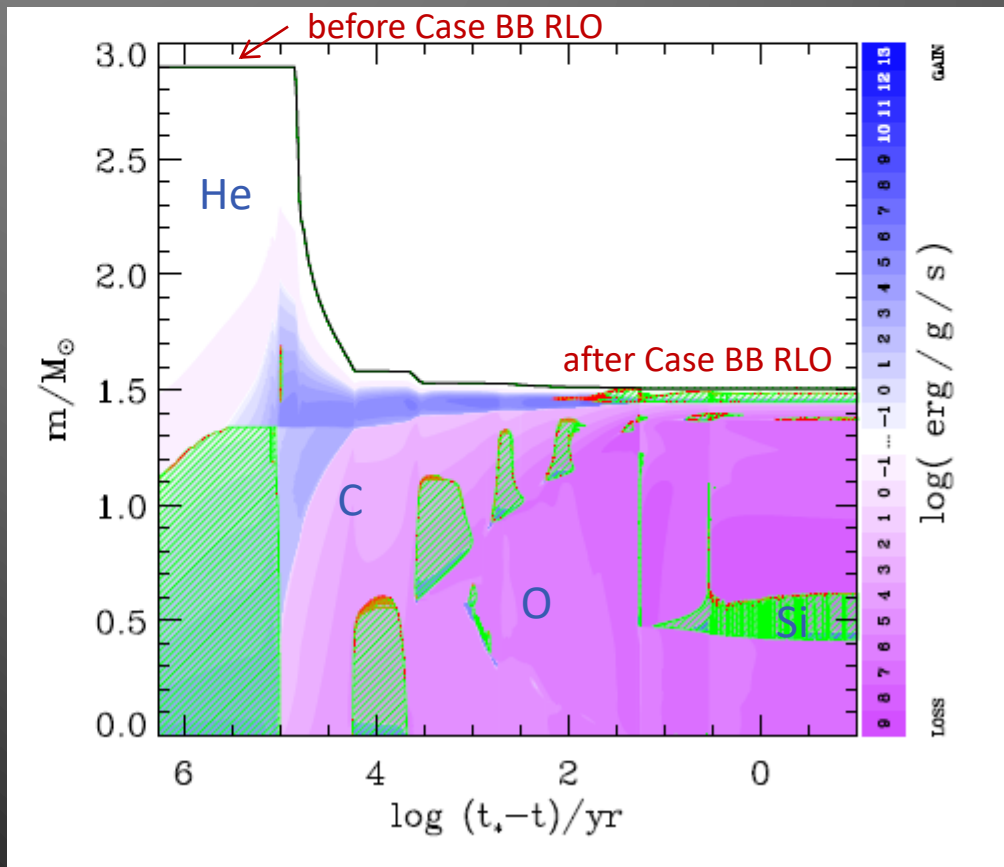
Tauris & Dewi (2001)



Ultra-stripped pre-SN metal core via Case BB RLO

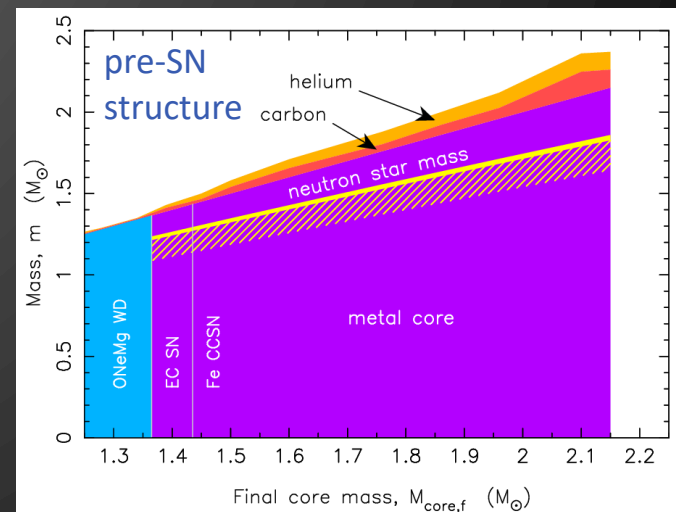


Tauris et al. (2013)



Post-CE evolution of He-star + NS in close orbit:
Case BB RLO strips off He env.
⇒ bare, pre-SN metal core just above Chandrasekhar mass

⇒ Iron core-collapse SN with very little ejecta + formation of low-mass NS in NS+NS system



Ultra-stripped pre-SN metal core via Case BB RLO

THE ASTROPHYSICAL JOURNAL LETTERS, 920:L36 (6pp), 2021 October 20

<https://doi.org/10.3847/2041-8213/ac2cc9>

© 2021. The American Astronomical Society. All rights reserved.



Novel Model of an Ultra-stripped Supernova Progenitor of a Double Neutron Star

Long Jiang^{1,2,3} , Thomas M. Tauris² , Wen-Cong Chen^{1,3} , and Jim Fuller⁴

¹ School of Science, Qingdao University of Technology, Qingdao 266525, People's Republic of China; chenwc@pku.edu.cn

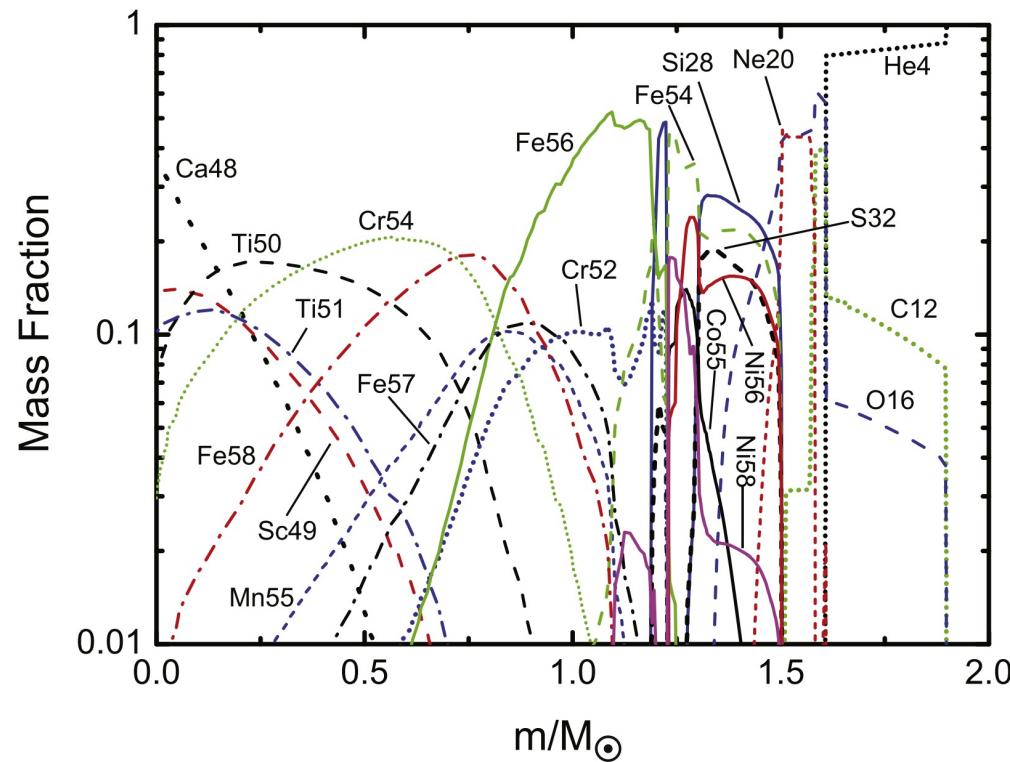
² Department of Physics and Astronomy, Aarhus University, Ny Munkegade 120, DK-8000 Aarhus C, Denmark

³ School of Physics and Electrical Information, Shangqiu Normal University, Shangqiu 476000, People's Republic of China

⁴ TAPIR, Mailcode 350-17, California Institute of Technology, Pasadena, CA 91125, USA

Received 2021 July 15; revised 2021 September 22; accepted 2021 October 5; published 2021 October 18

MESA



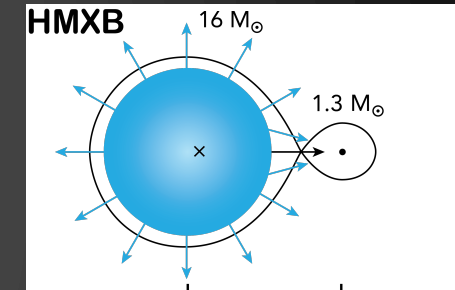
Intermediate-Mass X-ray Binaries

Why are so few IMXBs observed ?

HMXB: wind accretion (beginning atmospheric RLO)

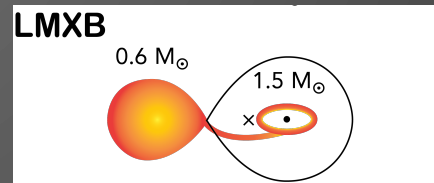
RLO is dynamically unstable and a CE forms

$$M_2 > 10 M_{\odot}$$



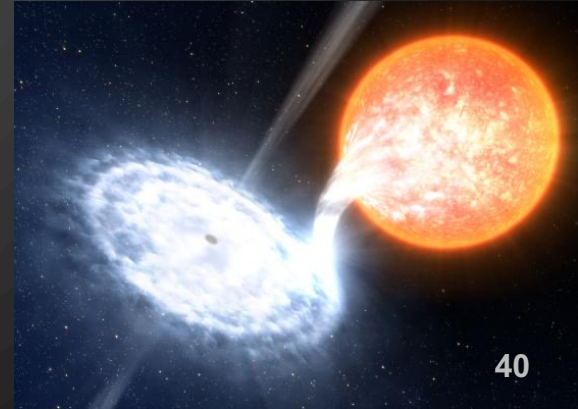
LMXB: stable RLO

$$M_2 \leq 1.5 M_{\odot}$$



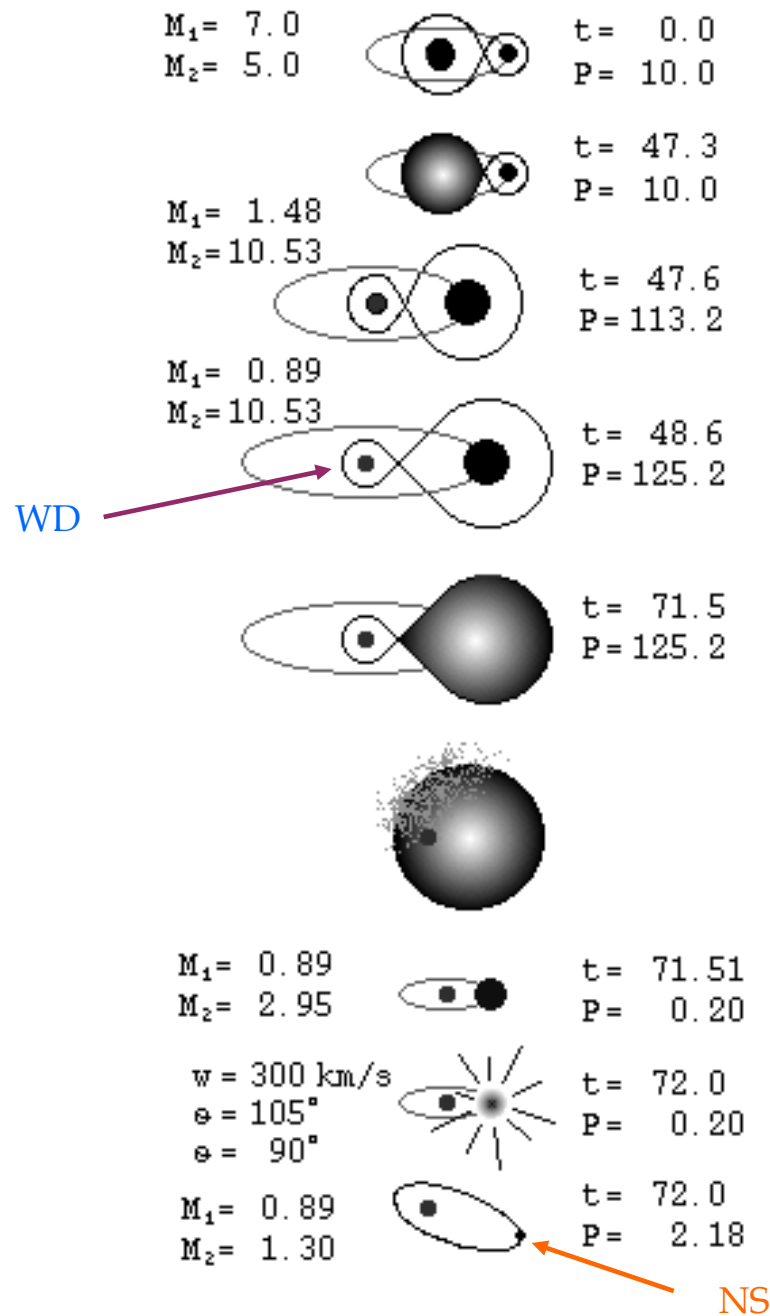
IMXB: wind accretion is too weak, and
RLO is often unstable (or very short)

But evidence of post-IMXBs
from pulsar+CO WD binaries



Double degenerate systems:

	<u>observed systems</u>	<u>X-ray progenitor systems</u>
WD+WD	(CO) WD + (CO) WD (AM CVn systems, RLO)	super-soft X-ray sources $M_2 > M_{WD}$ novae-like systems $M_2 < M_{WD}$
NS+WD	millisecond pulsars slow binary pulsars	LMXBs millisecond X-ray pulsars (SAX 1808.8-3658)
WD+NS	old WD + young pulsar (PSR 2303+46)	see next two slides with mass reversal
WD+BH	(not possible)	
NS+NS	recycled pulsar + young pulsar (PSR 1913+16, J0737-3039)	HMXBs (Vela X-1)
BH+WD	(no detections)	SXTs
BH+NS	BH + young pulsar (no detections)	HMXBs (Cyg X-1, LMC X-1)
NS+BH	semi-recycled pulsar + BH (no detections yet)	HMXBs (GX 301-2)
BH+BH	(only detectable via gwr)	HMXBs (MX33 X-7, IC10 X-1, NGC300 X-1)



Tauris & Sennels (1999)

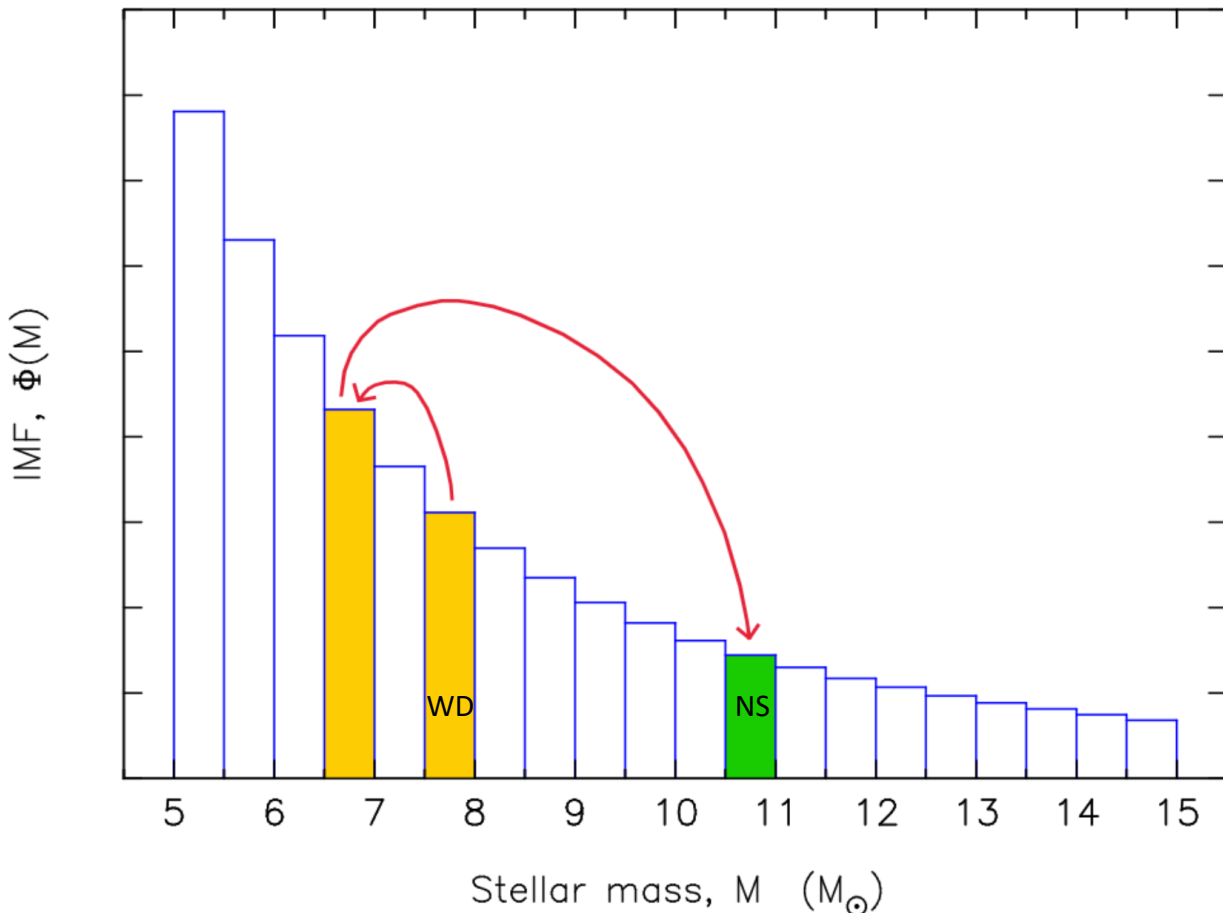
Binaries undergoing mass reversal

Tauris & van den Heuvel (2023)

producing (WD+NS) systems

first formed

second formed
(non-recycled, young,
eccentric orbit from SN)

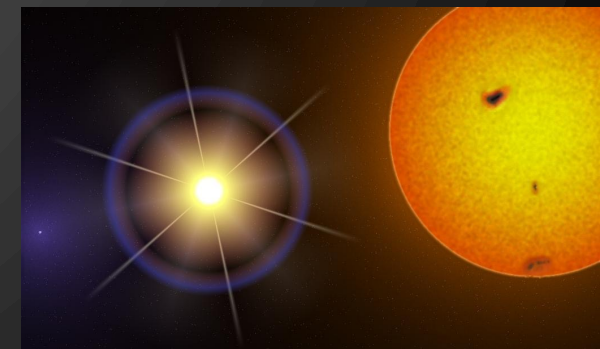


Dynamical effects of asymmetric SNe

As a result of non-radial hydrodynamical instabilities newborn NSs receive a momentum kick at birth (resulting in a kick velocity of $\sim 500 \text{ km s}^{-1}$).

The exact origin is still uncertain but is probably related to neutrino-driven convection bubbles, standing accretion shock instabilities (SASI) in the proto NS or other anisotropies in the ejecta which accelerate the proto-NS via the gravitational tug-boat mechanism, or simply an asymmetric neutrino outflow (see Janka 2012 for a review).

- As a consequence of the imparted kick radio pulsars have large velocities ($0\text{-}1000 \text{ km s}^{-1}$) and they have a wide scatter in their Galactic height distribution.
- Most (90%) of all potential LMXB systems are disrupted because of this kick.
- If SNe were purely symmetric then binary systems would be disrupted if $\Delta M/M > \frac{1}{2}$ (as a consequence of the virial theorem). Thus a kick can also help to keep systems bound if the direction of the kick is towards the companion star.



Dynamical effects of asymmetric SNe

is:

$$\frac{X_+}{A} = -\cos \beta \left[\xi \sin \gamma + (\xi - 1) \sqrt{\frac{\xi}{\xi - 2}} \right] \quad (38)$$

$$\frac{Y_+}{A} = \xi \cos^2 \gamma - 1 - \sin \gamma \sqrt{\frac{\xi}{\xi - 2}} \quad (39)$$

$$\frac{Z_+}{A} = -\sin \beta \sin \lambda \left[\xi \sin \gamma + (\xi - 1) \sqrt{\frac{\xi}{\xi - 2}} \right] \quad (40)$$

where we have used $u_\infty = A e^2$ and $u_0 = u_\infty \sqrt{\xi}/(\xi - 2)$.

We now proceed to express β , γ and λ in the true input angles ϑ and φ . We cannot reach $\sin \lambda$ directly, but that doesn't matter, from Fig. 1 (bottom) we have: $u_0 \sin \beta \sin \lambda = w \sin \vartheta \sin \varphi$. Intermediate results are:

$$X_+ = \frac{v + w \cos \vartheta}{1 - \xi + \sqrt{\xi(\xi - 2)} \sin \gamma} \quad (41)$$

$$Y_+ = \frac{\sqrt{\xi(\xi - 2)}}{1 + \xi(\xi - 2) \cos^2 \gamma} \times \left[u_0 \left(1 - \frac{1}{\xi} \right) - \frac{1}{u_0} (w \sin \vartheta \cos \varphi - v_{\text{im}})^2 \right] \quad (42)$$

$$Z_+ = \frac{w \sin \vartheta \sin \varphi}{1 - \xi + \sqrt{\xi(\xi - 2)} \sin \gamma} \quad (43)$$

To shorten the expressions a little more, define:

$$P \equiv 1 - 2\tilde{m} + \frac{w^2}{v^2} + 2\frac{w}{v^2}(v \cos \vartheta - v_{\text{im}} \sin \vartheta \cos \varphi) \quad (44)$$

$$Q \equiv 1 + \frac{P}{\tilde{m}} - \frac{(w \sin \vartheta \cos \varphi - v_{\text{im}})^2}{\tilde{m}v^2} \quad (45)$$

$$R \equiv \left(\frac{\sqrt{P}}{\tilde{m}v} (w \sin \vartheta \cos \varphi - v_{\text{im}}) - \frac{P}{\tilde{m}} - 1 \right) \frac{1 + m_{2f}}{m_{2f}} \quad (46)$$

$$S \equiv \left(\frac{1 + Q}{\tilde{m}} \right) \frac{\text{Autumn 2023}}{m_{2f}} \quad (47)$$

$$R \quad J \quad m_{2f}$$

Inserting Eqs. (48)–(50) into Eqs. (12) and (13) gives the final velocities of the stellar components in the original reference frame.

We find for the neutron star:

$$v_{\text{NS},x} = w \cos \vartheta \left(\frac{1}{R} + 1 \right) + \left(\frac{1}{R} + \frac{m_2}{1 + m_{\text{shell}} + m_2} \right) v \quad (51)$$

$$v_{\text{NS},y} = w \sin \vartheta \cos \varphi \left(1 - \frac{1}{S} \right) + \frac{1}{S} v_{\text{im}} + \frac{Q\sqrt{P}}{S} v \quad (52)$$

$$v_{\text{NS},z} = w \sin \vartheta \sin \varphi \left(\frac{1}{R} + 1 \right) \quad (53)$$

and for the companion star:

$$v_{2x} = \frac{-w \cos \vartheta}{m_{2f} R} - \left(\frac{1}{m_{2f} R} + \frac{1 + m_{\text{shell}}}{1 + m_{\text{shell}} + m_2} \right) v \quad (54)$$

$$v_{2y} = \frac{w \sin \vartheta \cos \varphi}{m_{2f} S} + \left(1 - \frac{1}{m_{2f} S} \right) v_{\text{im}} - \frac{Q\sqrt{P}}{m_{2f} S} v \quad (55)$$

$$v_{2z} = \frac{-w \sin \vartheta \sin \varphi}{m_{2f} R} \quad (56)$$

3. Results

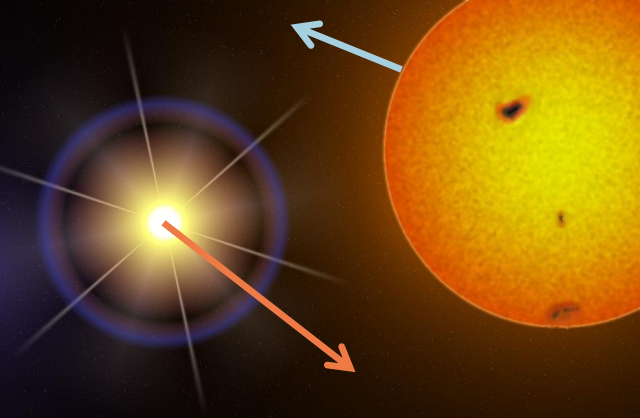
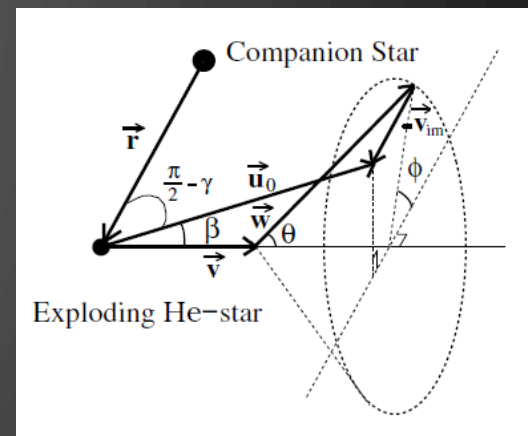
In the following subsection (Sect. 3.1) we briefly describe a few general consequences on the binary systems as a result of an asymmetric SN. In Sect. 3.2 we discuss the influence of the pre-SN orbital parameters on the velocities of neutron stars ejected from disrupted binaries. Sect. 3.3 briefly demonstrates applications to systems which either undergo a symmetric SN or remain bound after the SN event.

3.1. Consequences of an asymmetric SN in a binary system

3.1.1. Direction of the kick and coalescence

First of all, we illustrate how the direction of the kick, imparted to the newborn neutron star, affects the velocity (speed) of the ejected neutron star. This is demonstrated in Fig. 4 (top) as a function of the pre-SN separation, r . We have assumed a mass of $M_1 = 4.0 M_\odot$ for the exploding He-star, a neutron star mass of $M_{\text{NS}} = 1.4 M_\odot$, a companion star mass of $M_2 = 1.0 M_\odot$

Runaway velocities of ejected stars
(Tauris & Takens, 1998)



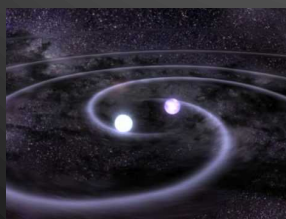
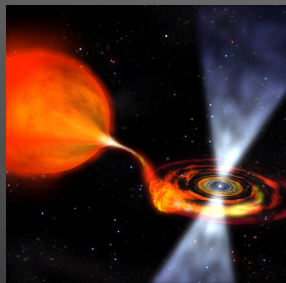
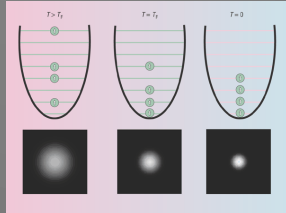
X-ray Binaries



- X-ray binaries (HMXBs / LMXBs)
- Roche-lobe overflow - Cases A, B, C, and Case BB
- Stability criteria for mass transfer / stellar evolution
- Orbital angular momentum balance equation
- Common envelope and spiral-in evolution

For a review: **Tauris & van den Heuvel (2006)**
and new textbook: **Tauris & van den Heuvel (2023)**

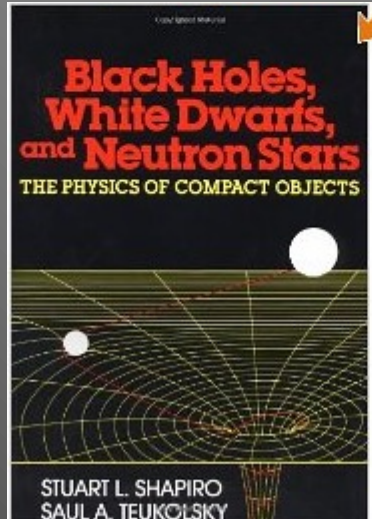
Programme



- * **Introduction**
- * **Degenerate Fermi Gases**
 - Non-relativistic and extreme relativistic electron / (n,p,e⁻) gases
- * **White Dwarfs**
 - Structure, cooling models, observations
- * **Neutron Stars**
 - Structure and equation-of-state
- * **Radio Pulsars**
 - Characteristics, spin evolution, magnetars, observations
- * **Binary Evolution and Interactions**
 - X-ray binaries, accretion, formation of millisecond pulsars, recycling
- * **Black Holes**
 - Observations, characteristics and spins
- * **Gravitational Waves**
 - Sources and detection, kilonovae
- * **Exam**

Physics of Compact Objects

week 7



Shapiro & Teukolsky (1983), Wiley-Interscience

Curriculum

(Tauris & van den Heuvel (2023), Chapters 4,6,7,10,11
+ S&T Chapter 13+15)

- Next lecture: Tauris & van den Heuvel (2023), Chapters 7.3 + 14
(S&T Chapter 18). Aud.2.115.

Exercises: # 9–11, 16

- Monday Oct. 23, 10:15-12:00